

Inversion angle of phase-polarization curve of near-Earth asteroid (3200) Phaethon

YOSHIHARU SHINNAKA,^{1,2} TOSHIHIRO KASUGA,^{2,3} REIKO FURUSHO,^{4,2} DANIEL C. BOICE,⁵ TSUYOSHI TERAI,⁶
 HIROTOMO NODA,⁷ NORIYUKI NAMIKI,⁷ AND JUN-ICHI WATANABE⁸

¹*Laboratory of Infrared High-resolution Spectroscopy (LiH), Koyama Astronomical Observatory, Kyoto Sangyo University, Motoyama, Kamigamo, Kita-ku, Kyoto 603-8555, Japan*

²*National Astronomical Observatory of Japan, 2-21-1 Osawa, Mitaka, Tokyo 181-8588, Japan*

³*Department of Physics, Kyoto Sangyo University, Motoyama, Kamigamo, Kita-ku, Kyoto 603-8555, Japan*

⁴*Tsuru University, 3-8-1 Tahara, Tsuru, Yamanashi 402-0052, Japan*

⁵*Scientific Studies and Consulting, 171 Harmon Drive, San Antonio, TX 78209, USA*

⁶*Subaru Telescope, National Astronomical Observatory of Japan, 650 North A'ohoku Place, Hilo, HI 96720, USA*

⁷*Rise project, National Astronomical Observatory of Japan, 2-21-1 Osawa, Mitaka, Tokyo 181-8588, Japan*

⁸*Public Relation Center, National Astronomical Observatory of Japan, 2-21-1 Osawa, Mitaka, Tokyo 181-8588, Japan*

(Received 2017 August 7; Accepted 2017 August 16)

Submitted to ApJL

ABSTRACT

The linear polarization degree (referred to the scattering plane, P_r) as a function of the solar phase angle, α , of solar system objects is a good diagnostic to understand the scattering properties of their surface materials. We report P_r of Phaethon over a wide range of α from $19^{\circ}.1$ to $114^{\circ}.3$ in order to better understanding properties of its surface materials. The derived phase-polarization curve shows that the maximum of P_r , P_{\max} , is $>42.4\%$ at $\alpha > 114^{\circ}.3$, a value significantly larger than those of the moderate albedo asteroids ($P_{\max} \sim 9\%$). The phase-polarization curve classifies Phaethon as *B*-type in the polarimetric taxonomy, being compatible with the spectral property. We compute the geometric albedo, p_v , of 0.14 ± 0.04 independently by using an empirical slope-albedo relation, and the derived p_v is consistent with previous results determined from mid-infrared spectra and thermophysical modeling. We could not find a fit to the period in our polarimetric data in the range from 0 up to 7.208 hr (e.g., less than twice the rotational period) and found significant differences between our P_r during the 2017 approach to the Earth and that of the 2016. These results imply that Phaethon has a region with different properties for light scattering near its orbital pole.

Keywords: minor planets, asteroids: individual: (3200) Phaethon – minor planets, asteroids: general – techniques: polarimetric

1. INTRODUCTION

Asteroid (3200) Phaethon is an Apollo-type near-Earth asteroid with a diameter of $5.1 \pm 0.2\text{ km}$ and a rotational period of $3.603958 \pm 0.000002\text{ hr}$ (Hanuš et al. 2016). It has a large orbital inclination (22.2°) and small perihelion distance (0.14 au). The surface of Phaethon has a geometric albedo, p_v , of 0.122 ± 0.008 using a thermophysical model of its mid-infrared spectra (Hanuš et al. 2016). Phaethon is thought to

be a collisional family member of asteroid (2) Pallas (Lemaitre & Morbidelli 1994), and they found that the typical p_v of the members of the Pallas Collisional Family (PCF) is larger than that of other *B*-type asteroids excluding PCF (Lemaitre & Morbidelli 1994). Phaethon is also likely the parent body of the Geminid meteor shower because of their orbital association (Whipple 1983; Williams & Wu 1993; de León et al. 2010). Recently, the small brightening and comet-like tails of Phaethon observed near perihelion in 2009, 2010, and 2012 were found to be caused by small dust grains produced by thermal fracture and/or desiccation cracking of surface materials and released by the solar ra-

Corresponding author: Yoshiharu Shinnaka
 yoshiharu.shinnaka@cc.kyoto-su.ac.jp, yoshiharu.shinnaka@nao.ac.jp

diation pressure (Jewitt & Li 2010; Li & Jewitt 2013; Jewitt et al. 2013). Because these current mass-loss events are not sufficient to explain the activity of the Geminids (Li & Jewitt 2013), Phaethon probably released a large amount of dust particles in the past, possibly due to comet-like activity driven by water ice sublimation.

Because of its small perihelion distance, the surface temperature of Phaethon exceeds 1000 K (Ohtsuka et al. 2009; Boice 2017) and receives high solar radiation pressure near perihelion. These effects are expected to cause small grains with radius of <1 mm to be blown off its surface (Jewitt & Li 2010) and thermal metamorphism of surface materials. It is thought that its surface is covered by rocks with coarser grain size and contains hydrated minerals from various observational, experimental, and theoretical studies (Licandro et al. 2007; de León et al. 2010; Hanuš et al. 2016). The linear polarization degree referred to the scattering plane, P_r (Zellner & Gradie 1976), as a function of the solar phase angle, α (i.e., Sun-object-observer angle) is a good diagnostic to understand the scattering properties of surface materials. Here we call this relation the 'phase-polarization curve'. The P_r in the large α region is controlled primarily by the properties of individual particles in the medium (Hapke 2012). Anyway, at the lower phase angle region (at $\alpha < \sim 40^\circ$), the phase-polarization curve has been used for the polarimetric classification for asteroids (Belskaya et al. 2017) and estimation of a geometric albedo, p_v (Cellino et al. 2015). Recent polarimetric results in the positive polarization branch of Phaethon during the 2016 and 2017 approach to the Earth suggest that Phaethon has an extremely high P_r compared to other solar system bodies (Ito et al. 2018; Devogéle et al. 2018); however, there was no measurement of P_r of Phaethon around the inversion angle ($\alpha < 30^\circ$).

2. OBSERVATIONS AND DATA REDUCTION

The polarimetric survey of Phaethon was performed for 13 consecutive nights from UT 2017 December 9 to December 21 using the Polarimetric Imager for Comets (PICO; Ikeda et al. 2007) mounted on the 50-cm Telescope for Public Outreach¹ at Mitaka Campus of National Astronomical Observatory of Japan. We used the standard Johnson-Cousins R_C -band filter (its bandpass is 483–799 nm; Bessell 2005) for all observations of Phaethon. Due to favourable weather conditions, we obtained a high-quality data set in the range of solar phase angle from $19^\circ.12$ through $114^\circ.30$ (Table 1).

The ranges of heliocentric and geocentric distances of Phaethon were 1.13–0.94 au and 0.15–0.07 au, respectively. The elevation of all observations was over 28° . Finally, 3,560 frames (890 sequences) of Phaethon were acquired during the survey. We excluded frames where stationary field stars and cosmic-rays overlapped Phaethon as judged by eye, leaving 3,248 frames (812 sequences) that were analysed. Details of PICO with the 50-cm telescope are described in Appendix A.

All selected PICO data were reduced using the standard reduction procedure for imaging observations of a point-source object (dark subtraction, flat-fielding, aperture photometry with the APPHOT package) described in Ikeda et al. (2007) with custom PyRAF script that uses IRAF² via Python developed by our group. We also applied a moving-circular aperture to photometry of Phaethon with an elongated shape on the images taken under sidereal tracking on 2017 December 17 (developed by Yoshida & Terai 2017). To calibrate the instrumental polarizations, we also observed unpolarized standard stars, completely polarized light obtained through a Glan-Taylor prism, and strong polarized standard stars. The degree of linear polarization, P , and the position angle, θ , from normalized Stokes parameters, q ($\equiv Q/I$) and u ($\equiv U/I$), are converted by the following expressions (Tinbergen 1996): $P = \sqrt{q^2 + u^2}$ and $\theta = \frac{1}{2} \arctan(u/q)$. Details of the polarization calibrations, correction of instrumental polarizations, and error estimations are described in Appendix B and Kawabata et al. (1999).

In general, the degree of linear polarization, P_r , and position angle, θ_r , in the scattering plane (the plane containing the object, the Sun, and the Earth at the time of observation) have been used to compare with other solar system objects. P_r and θ_r are expressed in $P_r = P_{\text{cel}} \cos(2\theta_{\text{cel}})$ and $\theta_r = \theta_{\text{cel}} - (\phi \pm 90^\circ)$, respectively, where ϕ is the position angle of the scattering plane and the sign is chosen to satisfy $0^\circ \leq (\phi \pm 90^\circ) \leq 180^\circ$ (Chernova et al. 1993). P_{cel} and θ_{cel} are linear polarization degree and polarization position angle in celestial coordinates, respectively. Position angles in the scattering plane at the mid-time of each sequence were calculated using JPL's HORIZONS system³. The resultant weighted mean of P_r and θ_r on each date was computed and is summarized in Table 2.

² IRAF is distributed by the National Optical Astronomy Observatory, which is operated by the Association of Universities for Research in Astronomy (AURA) under a cooperative agreement with the National Science Foundation.

³ <https://ssd.jpl.nasa.gov/horizons.cgi>

¹ <https://www.nao.ac.jp/en/access/mitaka/facilities/50cm-telescope.html>

Table 1. Polarimetric results of Phaethon

UT Time in 2017	ϕ (°)	α (°)	T_{exp} (s × sequence)	Polarimetric standard stars
Dec 9 12:16:13–17:46:49	203.34–200.28	19.31– 19.21	30 × 93	HD 65583 (UP, GT), HD 204827 (SP)
Dec 10 10:58:02–16:57:46	189.85–185.70	19.12– 19.19	30 × 94	HD 65583 (UP, GT), HD 204827 (SP)
Dec 11 10:46:27–16:31:51	172.50–167.81	19.81– 20.19	30 × 99	HD 214923 (UP, GT), HD 204827 (SP)
Dec 12 12:20:02–16:32:54	151.07–147.33	22.28– 22.92	20 × 5 + 30 × 72	HD 432 (UP, GT), HD 204827 (SP)
Dec 13 10:15:17–15:12:28	131.90–127.55	26.43– 27.71	30 × 76	HD 214923 (UP, GT), HD 204827 (SP)
Dec 14 12:11:57–15:58:44	110.04–107.00	34.46– 35.95	30 × 60	HD 39587 (UP, GT)
Dec 15 09:10:53–11:01:58	115.53–112.38	43.30– 44.56	20 × 44	HD 39587 (UP, GT), HD 19820 (SP)
Dec 16 09:00:58–13:17:53	80.00– 77.93	56.68– 59.26	20 × 72 + 30 × 21	HD 39587 (UP, GT), HD 19820 (SP)
Dec 17 09:23:30–12:34:53	70.52– 69.66	71.50– 73.45	20 × 41	HD 39587 (UP), HD 432 (GT), HD 19820 (SP)
Dec 18 08:52:14–12:03:59	66.01– 65.68	85.18– 86.93	30 × 64	HD 39587 (UP, GT), HD 19820 (SP)
Dec 19 08:57:50–11:21:10	64.71– 64.70	97.11– 98.22	30 × 44	HD 39587 (UP, GT), HD 19820 (SP)
Dec 20 08:37:34–10:28:23	65.29– 65.39	106.54–107.19	60 × 20	HD 39587 (UP, GT), HD 19820 (SP)
Dec 21 08:48:10–09:48:26	66.83– 66.91	114.03–114.30	120 × 7	HD 154345 (UP, GT), HD 19820 (SP)

NOTE— UT date is the mid-time of the start and final sequences. ϕ and α are the angle of the scattering plane and the solar phase angle of the observations, respectively. T_{exp} is exposure time of each frame in seconds and number of sequences. UP, GT, and SP in the column of polarimetric standard stars indicate unpolarized standard stars, fully linear polarized light from the Glan-Taylor prism, and strong polarized standard stars, respectively; chosen from Serkowski (1974), Schmidt et al. (1992), and Wolff et al. (1996) for calibrating the instrumental polarization.

3. RESULTS AND DISCUSSION

We report the phase-polarization curve of Phaethon over a wide range of α from $19^\circ.1$ through $114^\circ.3$ and find that P_r grows steadily through α of 114° (Figure 1, Table 2). The expected maximum linear polarization degree, P_{max} , of Phaethon is $>42.4\%$ (3σ lower limit) and α_{max} , α at P_{max} , is located at $>114^\circ$. This value is consistent with other polarimetric observations of Phaethon (Ito et al. 2018; Devogéle et al. 2018). The derived P_{max} at α_{max} of Phaethon are more than four times larger than those values for the moderate albedo asteroids (e.g., $P_{\text{max}} < \sim 9\%$; Lupishko 2014; Ishiguro et al. 2017, at $\alpha_{\text{max}} \sim 100^\circ$; Geake & Dollfus 1986; Lupishko 2014), implying peculiar surface properties of Phaethon. To explain Phaethon’s large linear polarization degree, Ito et al. (2018) pointed out the interpretations: lower p_v than the current estimations, relatively large grains, and high surface porosity.

3.1. Polarimetric classification and geometric albedo

To derive an inversion angle, α_{inv} [°] at which P_r changes its sign, and a polarimetric slope at α_{inv} , h [% deg $^{-1}$], we computed the best-fit of the phase-polarization curve at $\alpha < 90^\circ$ using the trigonometrical function (Lumme & Muinonen 1993) by χ^2 minimization with the Marquardt-Levenberg algorithm (Press et al. 1992) (Figure 2). This trigonometrical function is given by $P_r(\alpha) = b \sin^{c_1}(\alpha) \sin^{c_2}(\alpha/2) \sin(\alpha -$

$\alpha_{\text{inv}})$, where b , α_{inv} , c_1 , and c_2 are free parameters. The trigonometrical function cannot be applied mathematically to polarimetric data when a phase-polarization curve has $\alpha > 110^\circ$ (Ishiguro et al. 2017), since there is no solution of $dP(\alpha)/d\alpha$ at $\alpha > 110^\circ$ with $c_2 > 0$, which $c_2 > 0$ is the original definition of this function (Lumme & Muinonen 1993). As a result, we applied the trigonometrical function with $c_2 < 0$ and used only limited polarimetric data at $\alpha < 90^\circ$. The derived best-fit parameters are $b = 21.33 \pm 0.44$, $\alpha_{\text{inv}} = 20^\circ.21 \pm 0^\circ.07$, $c_1 = 0.402 \pm 0.038$, and $c_2 = -1.57 \pm 0.07$, corresponding to $\alpha_{\text{inv}} = 20^\circ.21 \pm 0^\circ.07$ and $h = 0.174\% \pm 0.053\% \text{ deg}^{-1}$. The computed minimum P_r , P_{min} , and α at P_{min} , α_{min} , have large errors because there are no observations of P_r at $< 19^\circ$ in the polarimetric data set (Figure 2 and Table 1). The derived α_{inv} is consistent with that of Phaethon alone ($18^\circ.8 \pm 1^\circ.6$; Devogéle et al. 2018). We note that these fitting results are not complete in the large α region ($\alpha > 90^\circ$) because of the fitting function.

We find that Phaethon is likely to be a *B*-type asteroid as well as *M*- and *K*-type asteroids by comparing our derived α_{inv} and h to the polarimetric taxonomy (Table 3 of Belskaya et al. 2017). Phaethon is classified as a *B*-type asteroid by the spectral classification of asteroids (Bus & Binzel 2002; DeMeo et al. 2009). We also confirmed that the phase-polarization curve of Phaethon at $\alpha < 40^\circ$ shows a similar trend

Table 2. Polarimetric results of Phaethon

UT Time in 2017	JD - 2,458,000	r_H (au)	Δ (au)	α ($^{\circ}$)	P_r (%)	θ_r ($^{\circ}$)
Dec 9 12:16:13–17:46:49	97.011262– 97.249845	1.129–1.126	0.154–0.151	19.31– 19.21	-0.288 \pm 0.002	3.8 \pm 0.2
Dec 10 10:58:02–16:57:46	97.956968– 98.206782	1.115–1.111	0.139–0.135	19.12– 19.19	-0.217 \pm 0.002	177.0 \pm 0.3
Dec 11 10:46:27–16:31:51	98.948924– 99.188785	1.100–1.096	0.123–0.119	19.81– 20.19	-0.154 \pm 0.002	136.1 \pm 1.0
Dec 12 12:20:02–16:32:54	100.013912–100.189514	1.083–1.080	0.107–0.105	22.28– 22.92	0.652 \pm 0.002	86.7 \pm 0.1
Dec 13 10:15:17–15:12:28	100.927280–101.133657	1.068–1.065	0.095–0.092	26.43– 27.71	2.074 \pm 0.002	88.8 \pm 0.1
Dec 14 12:11:57–15:58:44	102.008299–102.165787	1.051–1.049	0.082–0.081	34.46– 35.95	4.593 \pm 0.003	88.6 \pm 0.1
Dec 15 09:10:53–11:01:58	102.882558–102.959699	1.037–1.036	0.075–0.074	43.30– 44.56	8.242 \pm 0.004	88.5 \pm 0.1
Dec 16 09:00:58–13:17:53	103.875671–104.054086	1.021–1.018	0.070–0.069	56.68– 59.26	15.453 \pm 0.004	88.6 \pm 0.1
Dec 17 09:23:30–12:34:53	104.891319–105.024225	1.004–1.002	0.069–0.070	71.50– 73.45	23.87 \pm 0.02	88.3 \pm 0.1
Dec 18 08:52:14–12:03:59	105.869606–106.002766	0.987–0.985	0.074–0.075	85.18– 86.93	31.71 \pm 0.01	88.7 \pm 0.1
Dec 19 08:57:50–11:21:10	106.873495–106.973032	0.970–0.969	0.082–0.083	97.11– 98.22	37.90 \pm 0.03	88.6 \pm 0.1
Dec 20 08:37:34–10:28:23	107.859421–107.936377	0.953–0.952	0.093–0.094	106.54–107.19	40.76 \pm 0.17	89.4 \pm 0.1
Dec 21 08:48:10–09:48:26	108.866782–108.908634	0.936–0.935	0.106–0.107	114.03–114.30	43.71 \pm 0.44	88.4 \pm 0.3

NOTE— UT date and JD are the mid-time of the start and final sequences. r_H and Δ are the heliocentric and geocentric distances in au and α is the solar phase angle. P_r and θ_r are the degree of linear polarization and polarization position angle referred to the scattering plane, respectively. The uncertainty in each value of P_r and θ_r includes both random errors (all sequences on each date and standard deviation of polarimetric standard stars during the survey) and the systematic error of PICO.

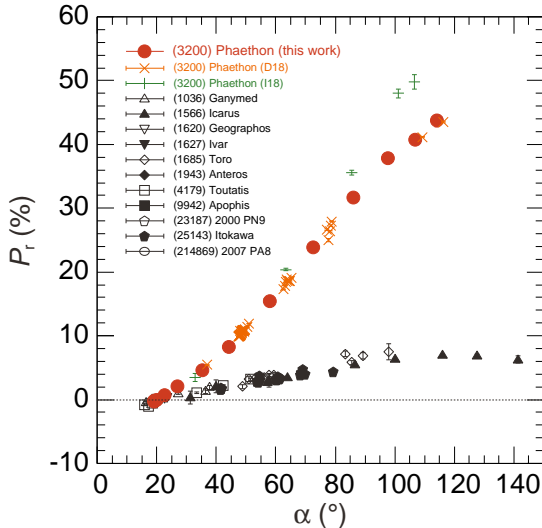


Figure 1. Phase-polarization curve of Phaethon in the R_C -band. Vertical and horizontal axes are the degree of linear polarization, P_r , and the solar phase angle, α , respectively. Red circles are the observed P_r of Phaethon at α on each date. The error bars are less than the symbol size, including both random errors (all sequences on each date and the standard deviation of polarization standard stars during the survey) and the systematic error of PICO. Orange crosses (D18) and green plus (I18) are the P_r of Phaethon taken on 2017 December (Devogéle et al. 2018) and during 2016 September–November (Ito et al. 2018), respectively. Black symbols are the P_r of the moderate albedo asteroids (Lupishko 2014; Ishiguro et al. 2017). The horizontal black dotted line shows $P_r = 0\%$.

to those of *B*- and *F*-type main-belt asteroids (Figure 4 of Gil-Hutton & García-Migani 2017). Regarding the polarimetric taxonomy, a behavior of P_r in the high- α region is unknown because mainly main-belt asteroids were used, which are difficult to acquire P_r in the high- α region from the ground-based observatories. Moreover, the derived α_{inv} is larger than and derived h is consistent with those of Pallas ($\alpha_{inv} = 18^{\circ}.1 \pm 0^{\circ}.1$ and $h = 0.228\% \pm 0.003\% \text{ deg}^{-1}$; Masiero et al. 2012). Belskaya et al. (2017) claimed that asteroids with much smaller α_{inv} have larger amount of regolith based on a relation between P_{min} and α_{inv} for asteroids of variable taxonomy types overlapped with lunar bare rocks and fines reported in Geake & Dollfus (1986). Based on this relation, Phaethon should have smaller grains on its surface compared with Pallas. On the other hand, Delbo et al. (2007) pointed out that much smaller bodies have less regolith or less mature regolith. It is expected that sizes of surface materials of Phaethon are larger than those of Pallas because the diameter of Phaethon (~ 5 km; Hanuš et al. 2016) is much smaller than that of Pallas (~ 500 km; Carry et al. 2010). This inconsistency implies that α_{inv} of an asteroid reflects scattering properties of grains (e.g., complex refractive index and grain size distribution) rather than a typical size of particles or rocks on the surface. Note that the relation between P_{min} and α_{inv} for asteroids may not be suitable for Phaethon because the P_r of the materials that were

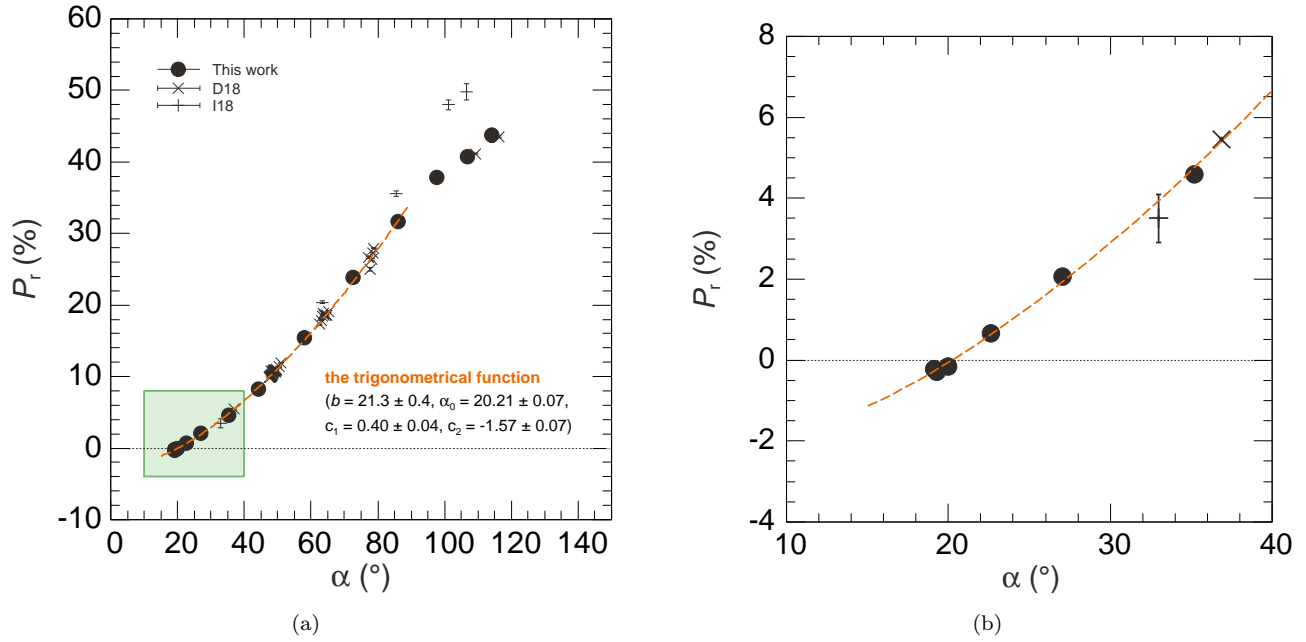


Figure 2. (a) The best-fit phase-polarization curve of Phaethon in the R_C -band at $\alpha < 90^\circ$. (b) Expanded figure near α_{inv} to show details (green hatch of panel (a)). Axes are identical to Figure 1. Black circles, cross, and plus symbols are the P_r of Phaethon in this work, D18 (Devogéle et al. 2018), and I18 (Ito et al. 2018), respectively. The dash (orange) lines indicate best-fit phase-polarization curve by the trigonometrical function (Lumme & Muinonen 1993). Note that the fitting result is not complete in the large α region ($\alpha > 90^\circ$) because P_r at $\alpha > 90^\circ$ are not used for these fittings (see Section 3.1).

investigated (e.g., Geake & Dollfus 1986; Belskaya et al. 2017) is significantly lower than that of Phaethon.

We estimate the p_v independently by using the empirical slope-albedo relation in the standard V -filter given by $\log_{10} p_v = C_1 \log_{10} h + C_2$, where h is the polarimetric slope at α_{inv} [% deg $^{-1}$]. C_1 and C_2 are constants ($C_1 = -0.80 \pm 0.04$ and $C_2 = -1.47 \pm 0.04$ when $p_v \geq 0.08$; Cellino et al. 2015). We apply this empirical relation to our polarimetric results in the R_C -band because no clear difference between P_r in the V - and R_C -bands of Phaethon have been reported (Devogéle et al. 2018). The derived p_v is equal to 0.14 ± 0.04 using our derived value of h ($0.174\% \pm 0.053\% \text{ deg}^{-1}$), corresponding to a moderate value among asteroids (Masiero et al. 2018). This value is consistent with a previous measurement of Phaethon determined from mid-infrared spectra and thermophysical modeling ($p_v = 0.122 \pm 0.008$; Hanuš et al. 2016), and may be high compared with typical cometary values (~ 0.04 ; Rickman 2017) claimed in Devogéle et al. (2018). This value is also consistent with B -type as well as M - and K -type asteroids (Belskaya et al. 2017). P_r in the low- α region ($\alpha < 15^\circ$) is required to derive other polarimetric parameters (e.g., P_{min} and α_{min}) and classify Phaethon in the polarimetric taxonomy.

To understand scattering properties of Phaethon's surface more deeply via reproducing its phase-polarization

curve, we require complex refractive index as well as size distribution of dominant surface materials. To derive an absorption coefficient of the complex refractive index, measurement of a circular polarization degree is theoretically useful (Hapke 2012). Mukai et al. (1987) demonstrated the importance of the negative as well as the positive branches of P_r to derive a typical complex refractive index of grain materials for comet 1P/Halley. Their result was based on the numerical calculations applying Mie theory and assuming a grain-size distribution obtained by the Vega mission (Mazets et al. 1987). We strongly encourage laboratory experiments to derive phase-polarization curves for various materials expected to exist on the surfaces of asteroids.

3.2. No confirmation of periodic change of P_r

Degewij et al. (1979) reported a variation in polarization degree in the B -band correlated with the lightcurve for (4) Vesta. The polarization variation was interpreted as albedo inhomogeneities of its surface materials (Degewij et al. 1979). Time-resolved polarimetry is an effective method to investigate albedo heterogeneity on asteroids. Panels (a)-(m) of Figure 3 show time-domain P_r of Phaethon during our polarimetric survey. We employed the phase dispersion minimization (PDM) method (Stellingwerf 1978) to search for periodicity in our polarimetric data, applying the 'cyclocode'

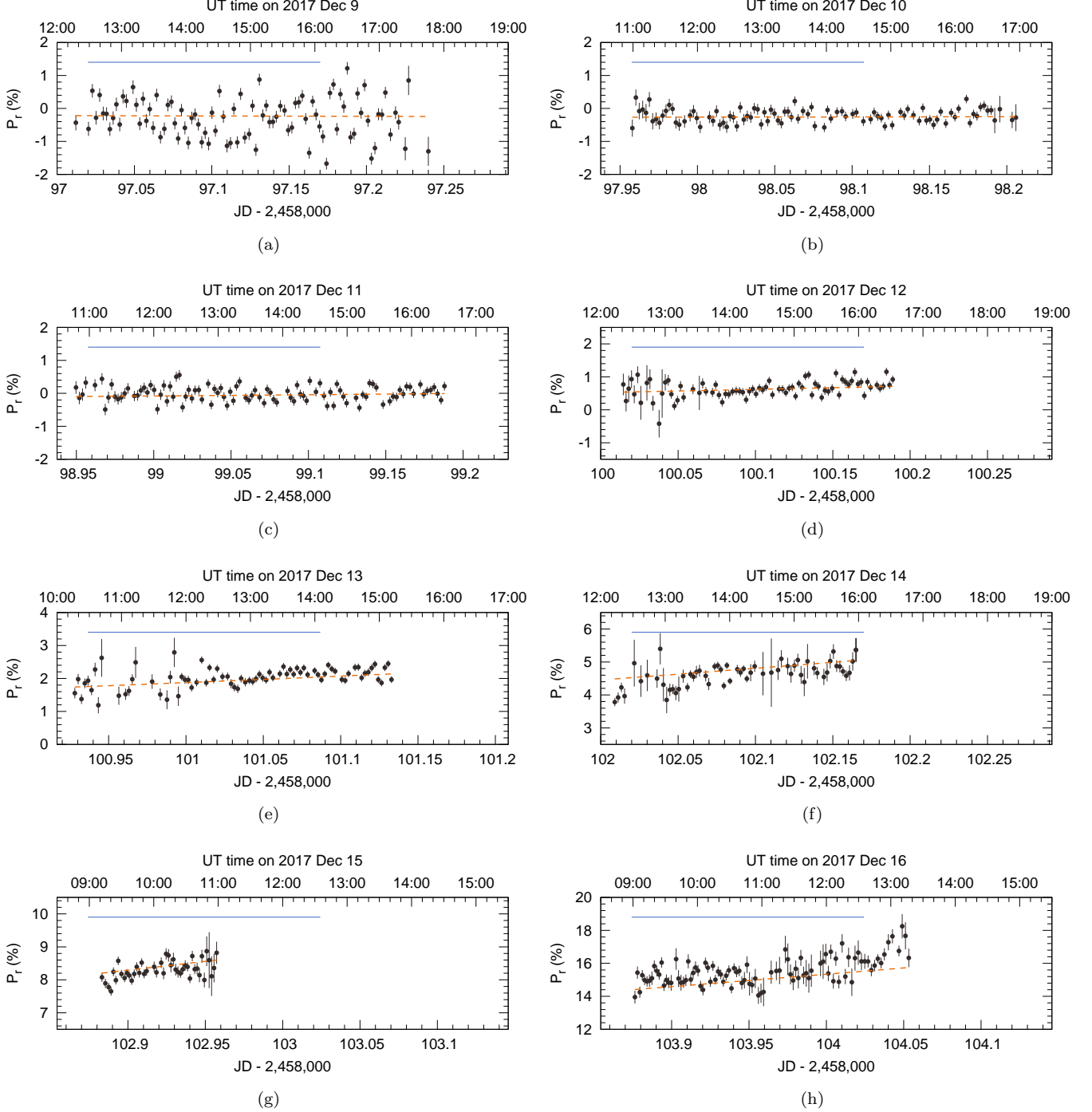
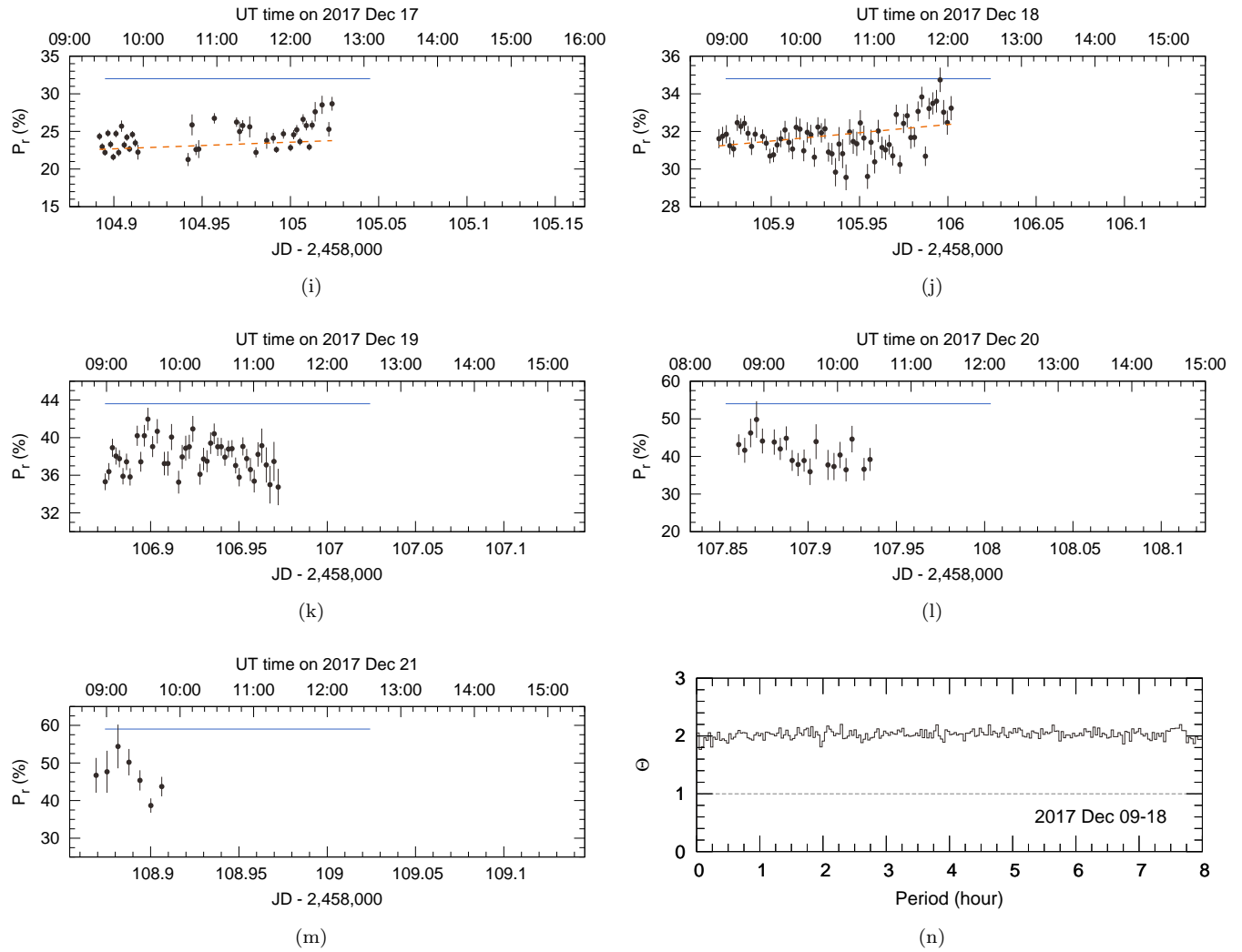


Figure 3. (a-m) Time-domain P_r of Phaethon from 2017 December 9 to December 21 and (n) the phase dispersion minimization plots for P_r of Phaethon from 2017 December 9 to 18. For panels (a) to (m), Black circles indicate P_r of Phaethon in each sequence in this work. The uncertainty of each plot includes both random and systematic errors described in Appendix B. The length of the upper horizontal (blue) bars indicate the rotational period of 3.604 hr. Orange dashed-lines in the panels of 2017 December 9-18 indicate phase-polarization fits using the trigonometrical function (Lumme & Muinonen 1993) in the range of $0^\circ < \alpha < 90^\circ$ (see section 3.1). The values and errors of each plot are listed in Table 3. For panel (n), vertical and horizontal axis are the dispersion of PDM, Θ , and the orbital period in hours, respectively. The horizontal gray dotted-line indicates $\Theta = 1.0$. We cannot find any best-fit period in the range from 0 up to 7.208 hr (e.g., less than twice the rotational period), since there is no orbital period with small Θ lower than 1.0.

**Figure 3.** *continued.*

software⁴. The best-fit period should have a very small normalized dispersion, Θ , compared with the unphased data, and thus $\Theta \ll 1$ indicates that a good fit has been found. To apply PDM fitting, we extract variable components from all P_r values until 2017 December 18 at $\alpha < 90^\circ$, with the best-fit phase-polarization curve derived by the trigonometrical function (see section 3.1 and Figure 3 (a-j)). Panel (n) of Figure 3 shows a PDM plot for variable components of P_r of Phaethon from 2017 December 9 to 18. We cannot find any good fit to the period in our polarimetric data (e.g., individual or combined dates from 2017 December 9 to 18), although Borisov et al. (2018) found a variation of P_r with rotation on 2017 December 15. Note that our polarimetric data on December 15 does not cover a complete period because of weather conditions. Using the pole orientation of $(\lambda_{\text{pole}}, \beta_{\text{pole}}) = (319^\circ, -39^\circ)$ with a 5° uncertainty (Hanuš et al. 2016), a surface region as seen from the Earth crossed from edge-on (perpendicular to pole direction) to the near north-pole direction during our survey by considering the positional relation between Earth and Phaethon at the time of these observations. Before 2017 December 18, we observed the edge-on direction (e.g., a different part of the surface at the rotational phase). This result suggests that surface materials on most regions of Phaethon have similar scattering properties (e.g., p_v).

Focusing on Phaethon's polarimetric results in the R_C -band, Figure 1 shows that our phase-polarization curve is significantly different in the high- α region ($\alpha > \sim 60^\circ$) with that during 2016 (Ito et al. 2018), although it is in agreement with that during 2016 in the low- α region (Ito et al. 2018) and during 2017 December

(Devogéle et al. 2018). Polarimetry in 2016 (Ito et al. 2018) observed only the edge-on direction (e.g., $\sim 80^\circ$ inclination of the north-pole direction seen from the Earth). In this case, materials causing lower polarization in the high- α regions by scattering are distributed near its rotational pole, and most surface regions (except for near the rotational pole region) have similar scattering properties. The difference of scattering properties on Phaethon's surface may reflect formation conditions in the early solar nebula and/or surface alternation after formation by the solar heating near perihelion. It is expected that not only determination of pole orientation but also the variation of scattering properties of materials with location on Phaethon's surface will be elucidated by detailed observations of the close flyby of Phaethon by the DESTINY⁺ mission (Sarli et al. 2018).

We are grateful to the staff of the Public Relation Center of the National Astronomical Observatory of Japan for their support during our observations. The authors sincerely thank Dr. Y. Ikeda, Prof. H. Kawakita, and Prof. M. Ishiguro for their valuable advice and comments. This research was supported by Grant-in-Aid for Japan Society for the Promotion of Science (JSPS) Fellows Grant No. 15J10864 (YS), JSPS KAKENHI Grant No. 17H06459 (NN), and National Science Foundation Planetary Astronomy Program (USA) Grant No. 0908529 (DCB). The transmittance of the standard Johnson-Cousins R_C -band filter made by TOPTEC (Czech Republic) was measured by using a UV-IR absorption spectrophotometer (Shimadzu, UV-3100PC) at the Advanced Technology Center of National Astronomical Observatory of Japan.

APPENDIX

A. POLARIMETRIC IMAGER FOR COMETS: PICO

PICO is a double-beam polarimetric imager with a calcite Wollaston prism and rotatable half-wave plate (Ikeda et al. 2007). It obtains a pair of polarized images simultaneously that are perpendicularly polarized rays (ordinary- and extraordinary-rays) split by the Wollaston prism. A commercial SBIG STL-1001E CCD camera was used as the detector. The array was cooled to -25°C within $\pm 0.1^\circ\text{C}$ by a two-stage thermoelectric system. Before our polarimetric survey of Phaethon on December 2017, we installed the standard Johnson-Cousins R_C filter made by TOPTEC (Czech Republic). When PICO is mounted on the 50-cm Telescope for Public Outreach (F/12.06), the typical pixel scale is $0''.82$ per pixel and the effective field-of-view of each polarized ray is $\sim 6'.2 \times 12'.9$ on the sky. To correct both a difference in transmittance of lenses used in PICO between ordinary- and extraordinary-rays and the time-dependent sky conditions, we obtained images at four different position angles of the half-wave plate (Kawabata et al. 1999). One set of exposures at these four different angles ($0^\circ, 45^\circ, 22^\circ.5, 67^\circ.5$) is called a sequence.

⁴ <http://www.toybox.rgr.jp/mp366/lightcurve/cyclocode/cyclocode.html>
developed by Dermawan (2004)

B. DERIVATION OF LINEAR POLARIZATION DEGREE

After extracting counts for the eight independent images (pairs of perpendicularly polarized images at four position angles of the half-wave plate), we calculate normalized Stokes parameters, q ($\equiv Q/I$) and u ($\equiv U/I$), of the i -th sequence in instrumental coordinates as follows:

$$q_{\text{inst}} \equiv \frac{Q(i)}{I(i)} = \frac{1 - a_1(i)}{1 + a_1(i)} \quad (\text{B1})$$

and

$$u_{\text{inst}} \equiv \frac{U(i)}{I(i)} = \frac{1 - a_2(i)}{1 + a_2(i)} \quad (\text{B2})$$

with

$$a_1(i) = \sqrt{\frac{I_{e,0^\circ}(i)/I_{o,0^\circ}(i)}{I_{e,45^\circ}(i)/I_{o,45^\circ}(i)}} \quad (\text{B3})$$

and

$$a_2(i) = \sqrt{\frac{I_{e,22.5^\circ}(i)/I_{o,22.5^\circ}(i)}{I_{e,67.5^\circ}(i)/I_{o,67.5^\circ}(i)}}, \quad (\text{B4})$$

where $I_{o,\Psi}$ and $I_{e,\Psi}$ are the ordinary and extraordinary intensities at the angle of the half-wave plate, Ψ , of the i -th sequence (Kawabata et al. 1999). In order to calibrate the instrumental polarizations (offset from the zero-point of q and u , instrumental depolarization, and offset in the position angle between the celestial and instrumental coordinates), we also observed unpolarized standard stars, completely polarized light obtained through a Glan-Taylor prism, and strong polarized standard stars. After calibrating the instrumental polarizations, the derived q and u with systematic mean errors are in celestial coordinates ($q_{\text{cel}} \pm \sigma_{q_{\text{cel}}}$ and $u_{\text{cel}} \pm \sigma_{u_{\text{cel}}}$). We obtain multiple sequences of Phaethon on each date and calculated the weighted mean of q_{cel} and u_{cel} on each date as given by

$$\overline{q_{\text{cel}}} = \frac{\sum_{i=1}^n (q_{\text{cel}}(i)/\sigma_{q_{\text{cel}}}(i))}{\sum_{i=1}^n (1/\sigma_{q_{\text{cel}}}(i))} \quad (\text{B5})$$

and

$$\overline{u_{\text{cel}}} = \frac{\sum_{i=1}^n (u_{\text{cel}}(i)/\sigma_{u_{\text{cel}}}(i))}{\sum_{i=1}^n (1/\sigma_{u_{\text{cel}}}(i))} \quad (\text{B6})$$

with an error of

$$\overline{\sigma_{q_{\text{cel}}}} = \sqrt{\frac{1}{\sum_{i=1}^n (1/\sigma_{q_{\text{cel}}}(i))}} \quad (\text{B7})$$

and

$$\overline{\sigma_{u_{\text{cel}}}} = \sqrt{\frac{1}{\sum_{i=1}^n (1/\sigma_{u_{\text{cel}}}(i))}}, \quad (\text{B8})$$

respectively. Here the degree of linear polarization, P , and the position angle, θ , from normalized Stokes parameters (q and u) are converted by the following expressions (Tinbergen 1996): $P = \sqrt{q^2 + u^2}$ and $\theta = \frac{1}{2}\tan(u/q)$. The systematic error of PICO was estimated to be $\delta P_{\text{sys}} = (P/85)\%$ over the entire field-of-view (Ikeda et al. 2007). More details of the polarization calibrations, correction of instrumental polarizations, and error estimations are described in Kawabata et al. (1999).

C. POLARIMETRIC RESULTS OF PHAETHON IN THE R_C -BAND

Table 3 is the time-domain summary of the polarimetric results of Phaethon in the R_C -band (812 sequences in total) taken by PICO polarimeter mounted on the 50-cm Telescope for Public Outreach at Mitaka Campus of National Astronomical Observatory of Japan.

REFERENCES

- Belskaya, I. N., Fornasier, S., Tozzi, G. P., et al., 2017, *Icarus*, 284, 30
- Bessell, M. S., 2015, *ARA&A*, 47, 293
- Boice, D. C., 2017, *J. Appl. Math. Phys.*, 4, 311
- Borisov, G., Devogéle, M., Cellino, A., et al., 2018, *Mon. Not. R. Astron. Soc.*, (astro-ph.1807.11842v1)
- Bus, S. J., Binzel, R. P. 2002, *Icarus*, 158, 146
- Carry, B., Dumas, C., Kaasalainen, M., et al. 2010, *Icarus*, 240, 472
- Cellino, A., Bagnulo S., Gil-Hutton, R., et al., 2005, *MNRAS*, 451, 3488
- Chernova, G. P., Kiselev, N. N., Jockers, K., 1993, *Icarus*, 103, 144
- Degewij, J., Tedesco, E. F., Zellner, B., 1979, *Icarus*, 40, 364
- Delbo, M., dell’Oro, A., Harris, A. W., Mottola, S., Mueller, M., 2007, *Icarus*, 190, 236
- de León, J., Campins, H., Tsiganis, K., Morbidelli, A., Licandro, J., 2010, *Astron.*
- DeMeo, F. E., Binzel, R. P., Slivan, S. M., Bus, S. J., 2009, *Icarus*, 202, 160
- Dermawan, B., 2004, Ph.D thesis, School of Science, University of Tokyo, pp. 118
- Devogéle, M., Cellino, A., , G., et al. 2018, *Mon. Not. R. Astron. Soc.*, 479, 3498
- Geake, J., Dollfus, A., 1986, *MNRAS*, 218, 75
- Gil-Hutton, R., García-Migani, E., 2017, *AAS Meeting Abstracts*, 607, A103
- Hanuš, J., Delbo’ M., Vokrouhlický, D., et al. *A&A*, 592, A34
- Hapke, B., 2012, *Theory of reflectance and emittance spectroscopy* (New York, Cambridge University Press)
- Ikeda, Y., Kawakita, H., Furusho, R., Sato, Y., Kasuga, T., 2007, *PASJ*, 59, 1017
- Ishiguro, M., Kuroda, D., Watanabe, M., et al., 2017, *AJ*, 154, 150
- Ito, T., Ishiguro, M., Arai, T., et al., 2018, *Nature Communications*, 9, 2486
- Jewitt, D., Li, J., Agarwal, J., 2013, *ApJL*, 771, L36
- Jewitt, D., Li, J., 2010, *AJ*, 140, 1519
- Kawabata, K., Okazaki, A., Akitaya, H., et al., 1999, *PASP*, 111, 898
- Li, J., Jewitt, D., 2013, *AJ*, 145, 154
- Lemaitre, A., Morbidelli, A., 1994, *Celest. Mech. Dyn. Astron.*, 60, 29
- Licandro, J., Campins, H., Mothé-Diniz, T., Pinilla-Alonso, N., de León, J., 2007, *Astron. Astrophys.*, 461, 751
- Lumme, K., Muinonen, K., 1993, *Proc. IAU Symposium*, 160, p194
- Lupishko, D., 2014, NASA Planetary Data System (Asteroid Polarimetric Database V8.0., Lupishko Eds.), EAR-A-3-RDR-APD-POLARIMETRY-V8.0.
- Masiero, J. R., Nugent, C., Mainzer, A. K., et al., 2018, *AJ*, 154, 168
- Masiero, J. R., Mainzer, A. K., Grav, T., et al., 2012, *ApJ*, 749, 104
- Mazets, E. P., Aptekar, R. L., Golenetskii, S. V., et al., 1986, *Nature*, 321, 276
- Mukai, T., Miyake, W., Terasawa, T., Kitayama, M., Hirao, K., 1987, *AAS Meeting Abstracts*, 187, 650
- Ohtsuka, K., Nakato, A., Nakamura, T., et al., 2009, *PASJ*, 61, 1375
- Press, W. H. et al. 1992, *Numerical Recipes in C: The Art of Scientific Computing* (2nd ed.; New York: Cambridge University Press)
- Rickman, H., Origin and Evolution of Comets: Ten Years after the Nice Model and One Year after Rosetta, (World Scientific Publishing Company) (2017) ISBN: 978-981-3222-58-8
- Sarli, B. V., Horikawa, M., Yam, C. H., Kawakatsu, Y., Yamamoto, T., 2018, *J. Astronaut Sci.*, 65, 82
- Schmidt, G. D., Elston, R., Lupie, O. L., 1992, *AJ*, 104, 1563
- Serkowski, K., 1974, *Methods in Experimental Physics: Astro-physics, Optical and Infrared*. 12, Part A., (N. Carleton, Eds., New York: Academic Press)
- Shepard, M. K., Clark, B. E., Nalan, M. C., et al., 2008, *Icarus*, 193, 20
- Stellingwerf, R., 1978, *ApJ*, 224, 953
- Tinbergen, J., 1996, *Astronomical Polarimetry* (Cambridge: Cambridge Univ. Press)
- Whipple, F. L., 1983, *IAU Circular*, 3881, 1
- Williams, I. P., Wu, Z., 1993, *MNRAS*, 262, 231
- Wolff, M. J., Nordsieck, K. H., Nook, M. A., 1996, *AJ*, 111, 856
- Yoshida, F., Terai, T., 2017, *AJ*, 154, 71

Zellner, B., Gradie, J., 1976, AJ, 81, 262

Table 3. Observational results acquired with PICO

UT Date	JD - 2,458,000	α ($^{\circ}$)	P_r (%)	θ_r ($^{\circ}$)
2017 Dec 9	97.0122	19.313	-0.43 \pm 0.23	155 \pm 10
2017 Dec 9	97.0203	19.309	-0.62 \pm 0.21	167 \pm 9
2017 Dec 9	97.0228	19.308	0.54 \pm 0.21	65 \pm 7
2017 Dec 9	97.0252	19.307	-0.28 \pm 0.21	30 \pm 11
2017 Dec 9	97.0275	19.306	0.41 \pm 0.21	79 \pm 13
2017 Dec 9	97.0298	19.304	-0.15 \pm 0.21	157 \pm 27
2017 Dec 9	97.0320	19.303	-0.16 \pm 0.20	142 \pm 8
2017 Dec 9	97.0341	19.302	-0.63 \pm 0.21	30.3 \pm 4.6
2017 Dec 9	97.0362	19.301	-0.29 \pm 0.20	31 \pm 9
2017 Dec 9	97.0384	19.300	0.13 \pm 0.20	120 \pm 23
2017 Dec 9	97.0405	19.299	-0.49 \pm 0.21	10 \pm 12
2017 Dec 9	97.0427	19.298	0.37 \pm 0.21	78 \pm 15
2017 Dec 9	97.0448	19.297	0.23 \pm 0.21	96 \pm 26
2017 Dec 9	97.0470	19.296	-2.03 \pm 0.21	173.9 \pm 2.9
2017 Dec 9	97.0491	19.295	0.65 \pm 0.21	113 \pm 6
2017 Dec 9	97.0513	19.294	0.11 \pm 0.21	48 \pm 6
2017 Dec 9	97.0534	19.293	-0.46 \pm 0.20	20 \pm 9
2017 Dec 9	97.0556	19.292	0.29 \pm 0.21	52.4 \pm 5.2
2017 Dec 9	97.0577	19.291	-0.38 \pm 0.20	164 \pm 13
2017 Dec 9	97.0599	19.290	-0.02 \pm 0.20	43 \pm 15
2017 Dec 9	97.0621	19.289	-0.59 \pm 0.20	5 \pm 10
2017 Dec 9	97.0644	19.288	0.41 \pm 0.19	75 \pm 12
2017 Dec 9	97.0669	19.287	-0.87 \pm 0.19	17.5 \pm 5.1
2017 Dec 9	97.0693	19.286	-0.62 \pm 0.19	157 \pm 6
2017 Dec 9	97.0717	19.285	0.11 \pm 0.19	133.5 \pm 2.8
2017 Dec 9	97.0739	19.284	0.20 \pm 0.19	125 \pm 9
2017 Dec 9	97.0761	19.283	-0.45 \pm 0.18	144.5 \pm 3.8
2017 Dec 9	97.0783	19.282	-0.91 \pm 0.19	161.2 \pm 4.7
2017 Dec 9	97.0805	19.281	-0.05 \pm 0.19	137 \pm 7
2017 Dec 9	97.0826	19.280	-0.59 \pm 0.20	24 \pm 6
2017 Dec 9	97.0848	19.278	-1.04 \pm 0.19	1.6 \pm 5.3
2017 Dec 9	97.0870	19.277	-0.29 \pm 0.19	33 \pm 7
2017 Dec 9	97.0892	19.277	-0.18 \pm 0.18	37 \pm 8
2017 Dec 9	97.0913	19.275	-0.48 \pm 0.18	3 \pm 11
2017 Dec 9	97.0935	19.274	-1.03 \pm 0.19	11.4 \pm 4.8
2017 Dec 9	97.0957	19.273	-0.74 \pm 0.19	13 \pm 6
2017 Dec 9	97.0980	19.272	-1.07 \pm 0.20	25.9 \pm 3.3
2017 Dec 9	97.1001	19.271	-0.13 \pm 0.19	38 \pm 10
2017 Dec 9	97.1024	19.270	-0.68 \pm 0.18	174 \pm 7

Table 3 continued

Table 3 (*continued*)

UT Date	JD - 2,458,000	α ($^{\circ}$)	P_r (%)	θ_r ($^{\circ}$)
2017 Dec 9	97.1050	19.269	0.53 ± 0.19	122.8 ± 4.3
2017 Dec 9	97.1075	19.268	-0.25 ± 0.19	146 ± 8
2017 Dec 9	97.1098	19.267	-1.13 ± 0.20	152.5 ± 2.9
2017 Dec 9	97.1121	19.266	-1.05 ± 0.18	7.0 ± 4.8
2017 Dec 9	97.1143	19.265	-0.01 ± 0.18	136 ± 16
2017 Dec 9	97.1165	19.264	-1.03 ± 0.18	173.2 ± 4.9
2017 Dec 9	97.1186	19.263	0.44 ± 0.18	74 ± 10
2017 Dec 9	97.1214	19.262	-0.88 ± 0.18	166.7 ± 5.2
2017 Dec 9	97.1242	19.260	-0.78 ± 0.18	16.9 ± 5.5
2017 Dec 9	97.1263	19.259	0.08 ± 0.18	123 ± 27
2017 Dec 9	97.1285	19.258	-1.25 ± 0.18	2.5 ± 4.2
2017 Dec 9	97.1308	19.257	0.88 ± 0.18	56.8 ± 2.4
2017 Dec 9	97.1331	19.256	-0.21 ± 0.18	151 ± 14
2017 Dec 9	97.1352	19.255	0.09 ± 0.18	46.3 ± 2.5
2017 Dec 9	97.1374	19.254	-0.41 ± 0.19	140.8 ± 2.7
2017 Dec 9	97.1396	19.253	-0.41 ± 0.19	13 ± 12
2017 Dec 9	97.1418	19.252	-0.25 ± 0.18	177 ± 20
2017 Dec 9	97.1443	19.251	0.08 ± 0.18	119 ± 35
2017 Dec 9	97.1470	19.250	-0.06 ± 0.18	140 ± 15
2017 Dec 9	97.1495	19.249	-0.66 ± 0.18	7 ± 7
2017 Dec 9	97.1518	19.248	-0.58 ± 0.18	17 ± 8
2017 Dec 9	97.1541	19.247	0.17 ± 0.18	122 ± 14
2017 Dec 9	97.1563	19.246	0.19 ± 0.18	123 ± 11
2017 Dec 9	97.1585	19.245	0.38 ± 0.18	117 ± 8
2017 Dec 9	97.1608	19.244	-0.31 ± 0.17	32 ± 7
2017 Dec 9	97.1630	19.243	-1.35 ± 0.18	173.9 ± 3.7
2017 Dec 9	97.1652	19.242	0.21 ± 0.17	128 ± 6
2017 Dec 9	97.1674	19.241	-0.19 ± 0.18	172 ± 27
2017 Dec 9	97.1697	19.240	-0.55 ± 0.18	32.0 ± 4.1
2017 Dec 9	97.1719	19.239	-0.85 ± 0.20	18 ± 5.3
2017 Dec 9	97.1741	19.238	-1.67 ± 0.18	7.8 ± 3.0
2017 Dec 9	97.1764	19.236	0.47 ± 0.19	60 ± 6
2017 Dec 9	97.1787	19.236	0.73 ± 0.17	96 ± 7
2017 Dec 9	97.1809	19.235	-0.63 ± 0.19	153.3 ± 5.1
2017 Dec 9	97.1832	19.233	0.43 ± 0.19	55.7 ± 4.5
2017 Dec 9	97.1854	19.233	0.06 ± 0.19	115 ± 61
2017 Dec 9	97.1876	19.232	1.22 ± 0.19	65.6 ± 2.9
2017 Dec 9	97.1898	19.231	-0.88 ± 0.20	155.0 ± 4.2
2017 Dec 9	97.1920	19.230	-0.77 ± 0.18	163.8 ± 5.7
2017 Dec 9	97.1943	19.229	0.45 ± 0.19	74 ± 10
2017 Dec 9	97.1966	19.228	-0.13 ± 0.18	144 ± 12

Table 3 continued

Table 3 (*continued*)

UT Date	JD - 2,458,000	α (°)	P_r (%)	θ_r (°)
2017 Dec 9	97.1988	19.227	0.71 ± 0.18	67.0 ± 5.1
2017 Dec 9	97.2010	19.226	-0.37 ± 0.18	22 ± 10
2017 Dec 9	97.2032	19.225	-1.52 ± 0.18	6.4 ± 3.3
2017 Dec 9	97.2055	19.224	-1.20 ± 0.19	161.7 ± 3.6
2017 Dec 9	97.2078	19.223	-0.17 ± 0.18	145 ± 10
2017 Dec 9	97.2100	19.222	-0.19 ± 0.18	39.9 ± 4.8
2017 Dec 9	97.2122	19.221	0.48 ± 0.18	111 ± 8
2017 Dec 9	97.2156	19.219	-0.79 ± 0.20	164 ± 6
2017 Dec 9	97.2188	19.218	-0.13 ± 0.19	40 ± 8
2017 Dec 9	97.2209	19.217	-0.41 ± 0.23	165 ± 14
2017 Dec 9	97.2251	19.215	-1.22 ± 0.35	12 ± 8
2017 Dec 9	97.2272	19.214	0.85 ± 0.44	64 ± 9
2017 Dec 9	97.2400	19.209	-1.30 ± 0.44	15 ± 9
2017 Dec 10	97.9579	19.118	-0.60 ± 0.26	166 ± 11
2017 Dec 10	97.9602	19.119	0.33 ± 0.25	106 ± 18
2017 Dec 10	97.9624	19.119	-0.08 ± 0.25	138 ± 9
2017 Dec 10	97.9646	19.120	-0.03 ± 0.27	41 ± 33
2017 Dec 10	97.9668	19.120	-0.13 ± 0.27	143 ± 16
2017 Dec 10	97.9689	19.121	0.27 ± 0.23	113 ± 17
2017 Dec 10	97.9711	19.121	-0.39 ± 0.25	177 ± 19
2017 Dec 10	97.9733	19.121	-0.32 ± 0.21	154 ± 11
2017 Dec 10	97.9754	19.122	-0.44 ± 0.19	1 ± 13
2017 Dec 10	97.9775	19.122	-0.22 ± 0.19	149 ± 12
2017 Dec 10	97.9797	19.123	-0.07 ± 0.19	140 ± 14
2017 Dec 10	97.9818	19.123	0.11 ± 0.19	96 ± 48
2017 Dec 10	97.9839	19.124	-0.01 ± 0.18	37 ± 122
2017 Dec 10	97.9861	19.124	-0.43 ± 0.19	7 ± 12
2017 Dec 10	97.9882	19.125	-0.49 ± 0.19	19 ± 8
2017 Dec 10	97.9917	19.125	-0.39 ± 0.19	5 ± 14
2017 Dec 10	97.9953	19.126	-0.21 ± 0.18	160 ± 19
2017 Dec 10	97.9975	19.126	-0.08 ± 0.18	172 ± 61
2017 Dec 10	97.9996	19.127	-0.29 ± 0.18	171 ± 17
2017 Dec 10	98.0018	19.127	-0.56 ± 0.18	2 ± 9
2017 Dec 10	98.0077	19.129	-0.26 ± 0.18	27 ± 12
2017 Dec 10	98.0101	19.129	-0.38 ± 0.17	172 ± 12
2017 Dec 10	98.0124	19.130	-0.08 ± 0.17	151 ± 32
2017 Dec 10	98.0145	19.130	-0.50 ± 0.17	2 ± 10
2017 Dec 10	98.0167	19.131	-0.43 ± 0.18	14 ± 11
2017 Dec 10	98.0189	19.131	-0.56 ± 0.18	173 ± 9
2017 Dec 10	98.0211	19.132	-0.23 ± 0.17	156 ± 14
2017 Dec 10	98.0232	19.132	-0.27 ± 0.17	160 ± 13

Table 3 continued

Table 3 (*continued*)

UT Date	JD - 2,458,000	α ($^{\circ}$)	P_r (%)	θ_r ($^{\circ}$)
2017 Dec 10	98.0255	19.133	-0.54 \pm 0.17	174 \pm 9
2017 Dec 10	98.0277	19.133	0.03 \pm 0.17	50 \pm 25
2017 Dec 10	98.0300	19.134	-0.34 \pm 0.17	166 \pm 13
2017 Dec 10	98.0323	19.134	-0.23 \pm 0.17	26 \pm 13
2017 Dec 10	98.0345	19.135	-0.27 \pm 0.17	156 \pm 12
2017 Dec 10	98.0367	19.136	0.01 \pm 0.16	134 \pm 24
2017 Dec 10	98.0390	19.136	-0.03 \pm 0.16	140 \pm 34
2017 Dec 10	98.0412	19.137	-0.48 \pm 0.16	164 \pm 8
2017 Dec 10	98.0433	19.137	-0.12 \pm 0.16	26 \pm 24
2017 Dec 10	98.0454	19.138	-0.39 \pm 0.16	175 \pm 11
2017 Dec 10	98.0475	19.138	-0.04 \pm 0.16	19 \pm 90
2017 Dec 10	98.0498	19.139	-0.15 \pm 0.16	145 \pm 10
2017 Dec 10	98.0521	19.139	-0.36 \pm 0.15	5 \pm 12
2017 Dec 10	98.0543	19.140	-0.45 \pm 0.15	168 \pm 9
2017 Dec 10	98.0564	19.140	-0.10 \pm 0.15	143 \pm 12
2017 Dec 10	98.0586	19.141	-0.09 \pm 0.15	175 \pm 46
2017 Dec 10	98.0607	19.142	-0.26 \pm 0.15	161 \pm 12
2017 Dec 10	98.0629	19.142	0.22 \pm 0.14	55 \pm 7
2017 Dec 10	98.0651	19.143	-0.32 \pm 0.14	169 \pm 12
2017 Dec 10	98.0683	19.143	-0.08 \pm 0.14	145 \pm 17
2017 Dec 10	98.0715	19.144	-0.17 \pm 0.14	16 \pm 21
2017 Dec 10	98.0737	19.145	0.04 \pm 0.14	61 \pm 51
2017 Dec 10	98.0759	19.146	-0.53 \pm 0.15	22 \pm 6
2017 Dec 10	98.0820	19.147	-0.58 \pm 0.14	162 \pm 6
2017 Dec 10	98.0841	19.148	-0.05 \pm 0.13	41 \pm 10
2017 Dec 10	98.0863	19.148	-0.31 \pm 0.14	17 \pm 11
2017 Dec 10	98.0902	19.149	-0.11 \pm 0.14	37 \pm 10
2017 Dec 10	98.0934	19.150	-0.09 \pm 0.14	23 \pm 32
2017 Dec 10	98.0958	19.151	-0.24 \pm 0.14	157 \pm 12
2017 Dec 10	98.1004	19.152	-0.17 \pm 0.15	171 \pm 24
2017 Dec 10	98.1027	19.153	-0.12 \pm 0.14	171 \pm 32
2017 Dec 10	98.1073	19.154	-0.39 \pm 0.15	9 \pm 10
2017 Dec 10	98.1120	19.156	-0.33 \pm 0.14	12 \pm 11
2017 Dec 10	98.1143	19.156	-0.12 \pm 0.14	142 \pm 8
2017 Dec 10	98.1166	19.157	-0.24 \pm 0.14	28 \pm 9
2017 Dec 10	98.1189	19.158	-0.29 \pm 0.13	155 \pm 9
2017 Dec 10	98.1212	19.158	-0.54 \pm 0.13	177 \pm 7
2017 Dec 10	98.1235	19.159	-0.20 \pm 0.13	26 \pm 12
2017 Dec 10	98.1259	19.160	-0.51 \pm 0.13	178 \pm 7
2017 Dec 10	98.1313	19.161	-0.11 \pm 0.13	17 \pm 29
2017 Dec 10	98.1337	19.162	-0.22 \pm 0.14	6 \pm 17

Table 3 continued

Table 3 (*continued*)

UT Date	JD - 2,458,000	α (°)	P_r (%)	θ_r (°)
2017 Dec 10	98.1360	19.163	-0.02 ± 0.13	42 ± 21
2017 Dec 10	98.1396	19.164	-0.20 ± 0.14	33 ± 8
2017 Dec 10	98.1434	19.165	-0.38 ± 0.14	21 ± 8
2017 Dec 10	98.1457	19.166	0.02 ± 0.14	126 ± 74
2017 Dec 10	98.1480	19.166	-0.37 ± 0.14	1 ± 11
2017 Dec 10	98.1503	19.167	-0.34 ± 0.13	164 ± 10
2017 Dec 10	98.1526	19.168	-0.50 ± 0.14	1 ± 8
2017 Dec 10	98.1550	19.169	-0.34 ± 0.13	2 ± 11
2017 Dec 10	98.1573	19.169	-0.10 ± 0.14	149 ± 19
2017 Dec 10	98.1606	19.170	-0.46 ± 0.13	166 ± 8
2017 Dec 10	98.1640	19.171	-0.13 ± 0.13	31 ± 14
2017 Dec 10	98.1665	19.172	-0.26 ± 0.13	12 ± 13
2017 Dec 10	98.1689	19.173	-0.01 ± 0.13	137 ± 42
2017 Dec 10	98.1739	19.175	0.29 ± 0.13	92 ± 13
2017 Dec 10	98.1762	19.175	-0.44 ± 0.13	178 ± 9
2017 Dec 10	98.1785	19.176	-0.17 ± 0.14	13 ± 21
2017 Dec 10	98.1807	19.177	-0.23 ± 0.14	166 ± 15
2017 Dec 10	98.1830	19.178	0.04 ± 0.14	132 ± 8
2017 Dec 10	98.1853	19.178	0.09 ± 0.14	70 ± 33
2017 Dec 10	98.1876	19.179	-0.06 ± 0.16	159 ± 51
2017 Dec 10	98.1899	19.180	-0.05 ± 0.14	143 ± 21
2017 Dec 10	98.1922	19.181	-0.36 ± 0.39	28 ± 16
2017 Dec 10	98.1955	19.182	-0.02 ± 0.40	136 ± 18
2017 Dec 10	98.2034	19.185	-0.35 ± 0.25	149 ± 10
2017 Dec 10	98.2059	19.186	-0.28 ± 0.41	160 ± 33
2017 Dec 11	98.9498	19.810	0.18 ± 0.19	110 ± 24
2017 Dec 11	98.9519	19.813	-0.14 ± 0.19	31 ± 18
2017 Dec 11	98.9540	19.816	-0.04 ± 0.19	41 ± 21
2017 Dec 11	98.9560	19.819	0.32 ± 0.19	71 ± 13
2017 Dec 11	98.9620	19.828	0.25 ± 0.18	82 ± 20
2017 Dec 11	98.9665	19.834	0.44 ± 0.17	99 ± 11
2017 Dec 11	98.9686	19.837	-0.49 ± 0.17	17.0 ± 8.4
2017 Dec 11	98.9707	19.840	-0.13 ± 0.18	147 ± 17
2017 Dec 11	98.9728	19.843	0.27 ± 0.17	95 ± 18
2017 Dec 11	98.9749	19.846	-0.10 ± 0.17	28 ± 27
2017 Dec 11	98.9770	19.850	-0.18 ± 0.17	164 ± 23
2017 Dec 11	98.9791	19.853	-0.12 ± 0.16	178 ± 38
2017 Dec 11	98.9812	19.856	0.00 ± 0.17	136 ± 24
2017 Dec 11	98.9833	19.859	0.15 ± 0.16	61 ± 16
2017 Dec 11	98.9875	19.865	-0.08 ± 0.16	140 ± 10
2017 Dec 11	98.9896	19.868	-0.06 ± 0.16	172 ± 69

Table 3 continued

Table 3 (*continued*)

UT Date	JD - 2,458,000	α ($^{\circ}$)	P_r (%)	θ_r ($^{\circ}$)
2017 Dec 11	98.9917	19.871	0.09 \pm 0.16	66 \pm 34
2017 Dec 11	98.9938	19.874	0.17 \pm 0.16	113 \pm 18
2017 Dec 11	98.9959	19.877	0.03 \pm 0.16	48 \pm 20
2017 Dec 11	98.9980	19.880	0.25 \pm 0.16	108 \pm 14
2017 Dec 11	99.0002	19.884	0.10 \pm 0.16	53 \pm 11
2017 Dec 11	99.0024	19.887	-0.48 \pm 0.16	178 \pm 9
2017 Dec 11	99.0045	19.890	-0.04 \pm 0.16	154 \pm 63
2017 Dec 11	99.0066	19.893	0.24 \pm 0.16	110 \pm 15
2017 Dec 11	99.0086	19.896	-0.24 \pm 0.16	7 \pm 19
2017 Dec 11	99.0106	19.899	0.21 \pm 0.16	88 \pm 21
2017 Dec 11	99.0126	19.902	-0.10 \pm 0.15	39 \pm 8
2017 Dec 11	99.0146	19.905	0.50 \pm 0.15	90 \pm 9
2017 Dec 11	99.0166	19.908	0.56 \pm 0.15	95 \pm 8
2017 Dec 11	99.0186	19.911	-0.42 \pm 0.15	180 \pm 10
2017 Dec 11	99.0206	19.914	-0.10 \pm 0.15	25 \pm 28
2017 Dec 11	99.0226	19.917	0.11 \pm 0.14	110 \pm 29
2017 Dec 11	99.0247	19.920	-0.16 \pm 0.14	153 \pm 15
2017 Dec 11	99.0267	19.924	0.09 \pm 0.14	113 \pm 30
2017 Dec 11	99.0291	19.927	0.10 \pm 0.14	77 \pm 35
2017 Dec 11	99.0311	19.930	-0.19 \pm 0.14	156 \pm 14
2017 Dec 11	99.0352	19.937	0.29 \pm 0.14	78 \pm 13
2017 Dec 11	99.0372	19.940	-0.35 \pm 0.14	23 \pm 8
2017 Dec 11	99.0393	19.943	0.13 \pm 0.14	112 \pm 21
2017 Dec 11	99.0413	19.946	0.01 \pm 0.14	49 \pm 40
2017 Dec 11	99.0434	19.949	0.16 \pm 0.14	74 \pm 21
2017 Dec 11	99.0454	19.952	-0.11 \pm 0.14	37 \pm 10
2017 Dec 11	99.0475	19.955	-0.37 \pm 0.14	161 \pm 9
2017 Dec 11	99.0495	19.959	0.05 \pm 0.14	110 \pm 64
2017 Dec 11	99.0515	19.962	-0.23 \pm 0.14	3.7 \pm 17
2017 Dec 11	99.0535	19.965	0.21 \pm 0.14	109 \pm 15
2017 Dec 11	99.0555	19.968	0.36 \pm 0.13	81 \pm 10
2017 Dec 11	99.0595	19.974	-0.14 \pm 0.13	148 \pm 13
2017 Dec 11	99.0615	19.977	-0.21 \pm 0.13	35 \pm 6
2017 Dec 11	99.0635	19.980	-0.06 \pm 0.14	154 \pm 36
2017 Dec 11	99.0655	19.984	0.10 \pm 0.14	109 \pm 32
2017 Dec 11	99.0684	19.988	-0.12 \pm 0.14	152 \pm 19
2017 Dec 11	99.0713	19.993	-0.30 \pm 0.14	15 \pm 11
2017 Dec 11	99.0734	19.996	0.13 \pm 0.14	121 \pm 15
2017 Dec 11	99.0754	19.999	0.02 \pm 0.13	133 \pm 16
2017 Dec 11	99.0775	20.003	-0.19 \pm 0.14	162 \pm 17
2017 Dec 11	99.0795	20.006	-0.28 \pm 0.14	25 \pm 9

Table 3 continued

Table 3 (*continued*)

UT Date	JD - 2,458,000	α (°)	P_r (%)	θ_r (°)
2017 Dec 11	99.0865	20.017	0.07 ± 0.14	54 ± 18
2017 Dec 11	99.0886	20.020	-0.13 ± 0.14	147 ± 12
2017 Dec 11	99.0906	20.023	-0.24 ± 0.14	149 ± 8
2017 Dec 11	99.0927	20.027	0.25 ± 0.14	76 ± 14
2017 Dec 11	99.0947	20.030	-0.03 ± 0.14	31 ± 69
2017 Dec 11	99.0968	20.033	-0.08 ± 0.14	139 ± 7
2017 Dec 11	99.0988	20.037	-0.23 ± 0.14	20 ± 13
2017 Dec 11	99.1009	20.040	0.38 ± 0.14	101 ± 10
2017 Dec 11	99.1049	20.046	0.04 ± 0.13	132 ± 8
2017 Dec 11	99.1075	20.051	0.31 ± 0.13	119 ± 7
2017 Dec 11	99.1101	20.055	-0.08 ± 0.13	148 ± 22
2017 Dec 11	99.1121	20.058	-0.39 ± 0.14	160 ± 8
2017 Dec 11	99.1142	20.062	0.04 ± 0.14	129 ± 22
2017 Dec 11	99.1163	20.065	-0.38 ± 0.13	162 ± 8
2017 Dec 11	99.1184	20.069	0.28 ± 0.13	72 ± 11
2017 Dec 11	99.1205	20.072	0.09 ± 0.13	111 ± 30
2017 Dec 11	99.1226	20.075	-0.10 ± 0.13	37 ± 10
2017 Dec 11	99.1247	20.079	-0.30 ± 0.13	37.6 ± 3.2
2017 Dec 11	99.1308	20.089	-0.14 ± 0.13	154 ± 17
2017 Dec 11	99.1330	20.093	-0.44 ± 0.12	168 ± 7
2017 Dec 11	99.1351	20.096	-0.04 ± 0.12	138 ± 9
2017 Dec 11	99.1373	20.100	-0.11 ± 0.12	176 ± 33
2017 Dec 11	99.1395	20.103	0.31 ± 0.13	123.9 ± 4.4
2017 Dec 11	99.1417	20.107	0.28 ± 0.13	95 ± 13
2017 Dec 11	99.1439	20.111	0.18 ± 0.13	79 ± 19
2017 Dec 11	99.1482	20.118	-0.34 ± 0.13	165 ± 10
2017 Dec 11	99.1526	20.125	-0.24 ± 0.14	147 ± 7
2017 Dec 11	99.1548	20.129	-0.10 ± 0.13	35 ± 14
2017 Dec 11	99.1569	20.133	-0.11 ± 0.13	37 ± 10
2017 Dec 11	99.1591	20.136	0.10 ± 0.13	58 ± 16
2017 Dec 11	99.1613	20.140	-0.02 ± 0.13	138 ± 15
2017 Dec 11	99.1635	20.144	0.21 ± 0.13	123 ± 7
2017 Dec 11	99.1657	20.147	0.19 ± 0.13	66 ± 13
2017 Dec 11	99.1679	20.151	-0.01 ± 0.13	139 ± 50
2017 Dec 11	99.1724	20.159	0.27 ± 0.13	66 ± 9
2017 Dec 11	99.1746	20.163	-0.03 ± 0.13	137 ± 10
2017 Dec 11	99.1768	20.166	0.08 ± 0.13	63 ± 29
2017 Dec 11	99.1790	20.170	0.10 ± 0.13	111 ± 27
2017 Dec 11	99.1812	20.174	0.19 ± 0.13	109 ± 16
2017 Dec 11	99.1834	20.178	-0.01 ± 0.14	160 ± 305
2017 Dec 11	99.1858	20.182	-0.21 ± 0.13	148 ± 8

Table 3 continued

Table 3 (*continued*)

UT Date	JD - 2,458,000	α ($^{\circ}$)	P_r (%)	θ_r ($^{\circ}$)
2017 Dec 11	99.1880	20.185	0.22 \pm 0.13	99 \pm 17
2017 Dec 12	100.0146	22.280	0.77 \pm 0.33	87 \pm 12
2017 Dec 12	100.0164	22.287	0.27 \pm 0.32	54 \pm 11
2017 Dec 12	100.0181	22.292	0.64 \pm 0.40	83 \pm 18
2017 Dec 12	100.0199	22.299	0.93 \pm 0.27	69 \pm 6
2017 Dec 12	100.0217	22.305	0.47 \pm 0.27	61 \pm 9
2017 Dec 12	100.0239	22.313	1.06 \pm 0.26	79 \pm 6
2017 Dec 12	100.0259	22.320	0.2 \pm 0.5	62 \pm 39
2017 Dec 12	100.0298	22.334	0.8 \pm 0.5	108 \pm 15
2017 Dec 12	100.0318	22.341	0.93 \pm 0.30	106 \pm 8
2017 Dec 12	100.0338	22.348	0.20 \pm 0.22	125 \pm 12
2017 Dec 12	100.0377	22.362	-0.42 \pm 0.42	174 \pm 28
2017 Dec 12	100.0397	22.369	0.5 \pm 0.7	60 \pm 21
2017 Dec 12	100.0417	22.376	0.83 \pm 0.25	106 \pm 7
2017 Dec 12	100.0437	22.383	0.89 \pm 0.16	78.6 \pm 4.9
2017 Dec 12	100.0456	22.390	0.47 \pm 0.14	95 \pm 8
2017 Dec 12	100.0476	22.397	0.12 \pm 0.13	61 \pm 17
2017 Dec 12	100.0496	22.404	0.29 \pm 0.14	113 \pm 10
2017 Dec 12	100.0516	22.411	0.72 \pm 0.15	88 \pm 6
2017 Dec 12	100.0536	22.418	0.38 \pm 0.15	67 \pm 8
2017 Dec 12	100.0596	22.440	0.62 \pm 0.15	92 \pm 7
2017 Dec 12	100.0637	22.454	0.51 \pm 0.52	86 \pm 31
2017 Dec 12	100.0659	22.462	0.80 \pm 0.15	97.9 \pm 5.1
2017 Dec 12	100.0680	22.470	0.55 \pm 0.13	75 \pm 6
2017 Dec 12	100.0722	22.485	0.53 \pm 0.14	99 \pm 7
2017 Dec 12	100.0743	22.492	0.76 \pm 0.13	96.0 \pm 4.7
2017 Dec 12	100.0764	22.500	0.45 \pm 0.13	85 \pm 8
2017 Dec 12	100.0785	22.508	0.23 \pm 0.13	87 \pm 16
2017 Dec 12	100.0807	22.515	0.48 \pm 0.13	74 \pm 7
2017 Dec 12	100.0828	22.523	0.47 \pm 0.13	77 \pm 7
2017 Dec 12	100.0852	22.532	0.55 \pm 0.13	92 \pm 7
2017 Dec 12	100.0876	22.541	0.58 \pm 0.12	87 \pm 6
2017 Dec 12	100.0897	22.548	0.57 \pm 0.12	94 \pm 6
2017 Dec 12	100.0918	22.556	0.53 \pm 0.12	96 \pm 6
2017 Dec 12	100.0940	22.564	0.31 \pm 0.12	83 \pm 11
2017 Dec 12	100.0961	22.572	0.56 \pm 0.13	89 \pm 7
2017 Dec 12	100.0983	22.580	0.63 \pm 0.13	96 \pm 6
2017 Dec 12	100.1004	22.587	0.48 \pm 0.12	85 \pm 7
2017 Dec 12	100.1025	22.595	0.66 \pm 0.12	90.4 \pm 5.3
2017 Dec 12	100.1046	22.603	0.60 \pm 0.12	89 \pm 6
2017 Dec 12	100.1068	22.611	0.69 \pm 0.12	80.1 \pm 4.7

Table 3 continued

Table 3 (*continued*)

UT Date	JD - 2,458,000	α (°)	P_r (%)	θ_r (°)
2017 Dec 12	100.1089	22.619	0.88 ± 0.12	90.7 ± 3.9
2017 Dec 12	100.1110	22.626	0.46 ± 0.12	89 ± 8
2017 Dec 12	100.1153	22.642	0.63 ± 0.12	87.8 ± 5.4
2017 Dec 12	100.1175	22.650	0.63 ± 0.12	90 ± 5.4
2017 Dec 12	100.1196	22.658	0.52 ± 0.12	73 ± 5.5
2017 Dec 12	100.1217	22.666	0.65 ± 0.12	92.6 ± 5.2
2017 Dec 12	100.1238	22.674	0.68 ± 0.12	79.9 ± 4.7
2017 Dec 12	100.1259	22.682	0.41 ± 0.12	93 ± 8
2017 Dec 12	100.1281	22.689	0.80 ± 0.12	90.2 ± 4.2
2017 Dec 12	100.1302	22.697	0.68 ± 0.12	96.9 ± 4.9
2017 Dec 12	100.1323	22.705	1.02 ± 0.12	89.3 ± 3.4
2017 Dec 12	100.1344	22.713	1.06 ± 0.12	87.6 ± 3.3
2017 Dec 12	100.1365	22.721	0.45 ± 0.12	77 ± 7
2017 Dec 12	100.1386	22.729	0.79 ± 0.13	75.7 ± 4
2017 Dec 12	100.1407	22.737	0.71 ± 0.12	82 ± 4.8
2017 Dec 12	100.1428	22.745	0.37 ± 0.13	121.5 ± 4.4
2017 Dec 12	100.1450	22.752	0.58 ± 0.13	99 ± 6
2017 Dec 12	100.1471	22.761	0.56 ± 0.13	103 ± 6
2017 Dec 12	100.1496	22.770	0.65 ± 0.13	91 ± 6
2017 Dec 12	100.1521	22.779	1.11 ± 0.13	82.1 ± 3.2
2017 Dec 12	100.1541	22.787	0.45 ± 0.13	76 ± 7
2017 Dec 12	100.1562	22.795	0.92 ± 0.13	94.5 ± 4.0
2017 Dec 12	100.1582	22.802	0.84 ± 0.13	89 ± 4.3
2017 Dec 12	100.1602	22.810	0.77 ± 0.13	77.3 ± 4.2
2017 Dec 12	100.1623	22.817	0.88 ± 0.13	96.9 ± 4.0
2017 Dec 12	100.1643	22.825	1.14 ± 0.13	91.7 ± 3.2
2017 Dec 12	100.1663	22.833	0.78 ± 0.12	81.4 ± 4.4
2017 Dec 12	100.1683	22.841	0.84 ± 0.12	97.4 ± 4.1
2017 Dec 12	100.1704	22.848	0.43 ± 0.13	68.0 ± 6.0
2017 Dec 12	100.1724	22.856	0.85 ± 0.13	76.7 ± 3.8
2017 Dec 12	100.1744	22.864	0.68 ± 0.12	70.2 ± 4.0
2017 Dec 12	100.1785	22.879	0.75 ± 0.12	91.7 ± 4.7
2017 Dec 12	100.1805	22.887	0.65 ± 0.12	85.5 ± 5.3
2017 Dec 12	100.1826	22.895	0.71 ± 0.12	72.4 ± 3.9
2017 Dec 12	100.1847	22.903	1.15 ± 0.12	87.5 ± 3.0
2017 Dec 12	100.1867	22.910	0.75 ± 0.12	102.1 ± 4.2
2017 Dec 12	100.1887	22.918	0.92 ± 0.12	81.0 ± 3.6
2017 Dec 13	100.9281	26.434	1.55 ± 0.16	94.3 ± 2.9
2017 Dec 13	100.9303	26.447	1.98 ± 0.16	86.0 ± 2.2
2017 Dec 13	100.9324	26.460	1.37 ± 0.15	88.1 ± 3.1
2017 Dec 13	100.9346	26.473	1.85 ± 0.15	89.1 ± 2.3

Table 3 continued

Table 3 (*continued*)

UT Date	JD - 2,458,000	α ($^{\circ}$)	P_r (%)	θ_r ($^{\circ}$)
2017 Dec 13	100.9367	26.485	1.93 ± 0.15	88.4 ± 2.2
2017 Dec 13	100.9390	26.499	1.65 ± 0.16	88.8 ± 2.7
2017 Dec 13	100.9412	26.512	2.27 ± 0.20	93.1 ± 2.7
2017 Dec 13	100.9434	26.525	1.19 ± 0.25	99 ± 6
2017 Dec 13	100.9455	26.537	2.6 ± 0.6	77.0 ± 5.4
2017 Dec 13	100.9566	26.604	1.48 ± 0.28	77.1 ± 5.0
2017 Dec 13	100.9610	26.630	1.52 ± 0.17	88.5 ± 3.2
2017 Dec 13	100.9631	26.643	1.62 ± 0.15	88.0 ± 2.7
2017 Dec 13	100.9653	26.656	1.98 ± 0.15	88.1 ± 2.2
2017 Dec 13	100.9675	26.669	2.5 ± 0.5	96.2 ± 6.1
2017 Dec 13	100.9781	26.733	1.90 ± 0.22	80.9 ± 3.1
2017 Dec 13	100.9834	26.765	1.51 ± 0.18	95.6 ± 3.3
2017 Dec 13	100.9877	26.791	1.36 ± 0.29	93 ± 7
2017 Dec 13	100.9898	26.804	2.04 ± 0.19	91.8 ± 2.9
2017 Dec 13	100.9925	26.820	2.79 ± 0.44	82.4 ± 3.8
2017 Dec 13	100.9951	26.836	1.46 ± 0.30	90.5 ± 5.2
2017 Dec 13	100.9973	26.849	2.05 ± 0.11	88.5 ± 1.6
2017 Dec 13	100.9994	26.862	1.96 ± 0.13	94.1 ± 1.9
2017 Dec 13	101.0015	26.875	1.95 ± 0.12	96.4 ± 1.8
2017 Dec 13	101.0036	26.888	1.72 ± 0.12	89.1 ± 2.0
2017 Dec 13	101.0069	26.908	1.88 ± 0.12	87.1 ± 1.8
2017 Dec 13	101.0102	26.928	2.56 ± 0.11	98.8 ± 1.2
2017 Dec 13	101.0131	26.946	1.87 ± 0.12	89.5 ± 1.8
2017 Dec 13	101.0152	26.959	2.33 ± 0.11	85.3 ± 1.4
2017 Dec 13	101.0179	26.976	1.97 ± 0.11	93.4 ± 1.6
2017 Dec 13	101.0202	26.990	2.30 ± 0.11	88.2 ± 1.4
2017 Dec 13	101.0236	27.011	2.05 ± 0.12	81.8 ± 1.7
2017 Dec 13	101.0269	27.031	2.06 ± 0.12	85.5 ± 1.7
2017 Dec 13	101.0291	27.045	1.84 ± 0.14	87.3 ± 2.2
2017 Dec 13	101.0313	27.059	1.73 ± 0.13	89.8 ± 2.0
2017 Dec 13	101.0335	27.072	1.68 ± 0.13	85.9 ± 2.2
2017 Dec 13	101.0356	27.085	2.00 ± 0.12	90.0 ± 1.7
2017 Dec 13	101.0383	27.102	1.89 ± 0.13	80.6 ± 1.8
2017 Dec 13	101.0410	27.119	1.94 ± 0.11	87.9 ± 1.7
2017 Dec 13	101.0432	27.132	1.91 ± 0.12	84.9 ± 1.7
2017 Dec 13	101.0453	27.146	1.99 ± 0.11	89.2 ± 1.6
2017 Dec 13	101.0475	27.159	2.13 ± 0.12	90.3 ± 1.6
2017 Dec 13	101.0496	27.172	2.01 ± 0.11	88.1 ± 1.6
2017 Dec 13	101.0518	27.186	1.95 ± 0.11	90.5 ± 1.6
2017 Dec 13	101.0540	27.200	2.19 ± 0.12	91.6 ± 1.6
2017 Dec 13	101.0562	27.214	2.02 ± 0.11	91.0 ± 1.6

Table 3 continued

Table 3 (*continued*)

UT Date	JD - 2,458,000	α (°)	P_r (%)	θ_r (°)
2017 Dec 13	101.0607	27.242	2.14 ± 0.11	87.6 ± 1.5
2017 Dec 13	101.0630	27.256	2.36 ± 0.11	91.7 ± 1.4
2017 Dec 13	101.0652	27.270	2.13 ± 0.11	89.7 ± 1.5
2017 Dec 13	101.0674	27.284	2.27 ± 0.11	89.7 ± 1.4
2017 Dec 13	101.0696	27.298	2.13 ± 0.11	89.6 ± 1.5
2017 Dec 13	101.0718	27.312	2.32 ± 0.10	92.3 ± 1.3
2017 Dec 13	101.0740	27.325	2.18 ± 0.10	93.9 ± 1.4
2017 Dec 13	101.0762	27.339	2.32 ± 0.10	86.4 ± 1.3
2017 Dec 13	101.0786	27.355	2.12 ± 0.10	88.0 ± 1.4
2017 Dec 13	101.0832	27.383	2.24 ± 0.10	91.0 ± 1.3
2017 Dec 13	101.0853	27.397	2.12 ± 0.10	91.1 ± 1.4
2017 Dec 13	101.0875	27.411	1.96 ± 0.10	85.1 ± 1.5
2017 Dec 13	101.0898	27.425	2.14 ± 0.10	88.6 ± 1.4
2017 Dec 13	101.0920	27.439	2.41 ± 0.10	88.9 ± 1.2
2017 Dec 13	101.0942	27.453	2.29 ± 0.10	90.5 ± 1.3
2017 Dec 13	101.0964	27.467	2.22 ± 0.10	88.1 ± 1.3
2017 Dec 13	101.1008	27.495	1.97 ± 0.10	89.5 ± 1.5
2017 Dec 13	101.1029	27.509	1.94 ± 0.10	86.2 ± 1.5
2017 Dec 13	101.1051	27.522	2.15 ± 0.11	91.3 ± 1.4
2017 Dec 13	101.1093	27.549	2.34 ± 0.11	88.5 ± 1.4
2017 Dec 13	101.1114	27.563	2.34 ± 0.11	92.4 ± 1.4
2017 Dec 13	101.1136	27.577	2.02 ± 0.11	87.9 ± 1.6
2017 Dec 13	101.1157	27.590	2.16 ± 0.11	90.2 ± 1.5
2017 Dec 13	101.1179	27.604	2.19 ± 0.11	87.7 ± 1.5
2017 Dec 13	101.1200	27.618	2.32 ± 0.11	89.8 ± 1.3
2017 Dec 13	101.1222	27.632	2.43 ± 0.11	89.0 ± 1.3
2017 Dec 13	101.1243	27.645	1.97 ± 0.11	85.7 ± 1.5
2017 Dec 13	101.1264	27.659	1.87 ± 0.11	91.6 ± 1.6
2017 Dec 13	101.1286	27.673	2.33 ± 0.10	90.9 ± 1.3
2017 Dec 13	101.1307	27.687	2.45 ± 0.10	93.0 ± 1.2
2017 Dec 13	101.1328	27.701	1.97 ± 0.10	89.6 ± 1.5
2017 Dec 14	102.0091	34.465	3.78 ± 0.13	91.2 ± 1.0
2017 Dec 14	102.0112	34.485	3.93 ± 0.15	87.7 ± 1.1
2017 Dec 14	102.0134	34.505	4.23 ± 0.14	88.5 ± 1.0
2017 Dec 14	102.0154	34.524	3.97 ± 0.23	90.1 ± 1.7
2017 Dec 14	102.0216	34.582	5.0 ± 0.7	91.3 ± 4.1
2017 Dec 14	102.0260	34.622	4.4 ± 0.5	85.9 ± 3.1
2017 Dec 14	102.0301	34.660	4.6 ± 0.5	80.3 ± 2.8
2017 Dec 14	102.0364	34.719	4.50 ± 0.28	86.9 ± 1.8
2017 Dec 14	102.0385	34.738	5.4 ± 0.5	85.5 ± 2.5
2017 Dec 14	102.0405	34.758	4.3 ± 0.5	83.4 ± 3.3

Table 3 continued

Table 3 (*continued*)

UT Date	JD - 2,458,000	α ($^{\circ}$)	P_r (%)	θ_r ($^{\circ}$)
2017 Dec 14	102.0426	34.777	3.85 \pm 0.40	89.4 \pm 3.1
2017 Dec 14	102.0446	34.796	4.15 \pm 0.19	89.9 \pm 1.3
2017 Dec 14	102.0466	34.815	4.18 \pm 0.15	87.8 \pm 1.0
2017 Dec 14	102.0485	34.833	4.06 \pm 0.22	88.8 \pm 1.5
2017 Dec 14	102.0505	34.851	4.18 \pm 0.38	88.1 \pm 2.6
2017 Dec 14	102.0533	34.877	4.57 \pm 0.20	87.6 \pm 1.2
2017 Dec 14	102.0561	34.903	4.23 \pm 0.13	88.9 \pm 0.9
2017 Dec 14	102.0580	34.922	4.63 \pm 0.12	89.0 \pm 0.7
2017 Dec 14	102.0600	34.940	4.55 \pm 0.15	89.4 \pm 0.9
2017 Dec 14	102.0619	34.958	4.70 \pm 0.19	86.9 \pm 1.2
2017 Dec 14	102.0638	34.977	4.73 \pm 0.18	89.5 \pm 1.1
2017 Dec 14	102.0678	35.014	4.58 \pm 0.17	89.2 \pm 1.1
2017 Dec 14	102.0698	35.032	4.33 \pm 0.18	87.4 \pm 1.2
2017 Dec 14	102.0737	35.069	4.86 \pm 0.12	90.2 \pm 0.7
2017 Dec 14	102.0756	35.088	4.89 \pm 0.12	88.4 \pm 0.7
2017 Dec 14	102.0776	35.106	4.77 \pm 0.12	87.0 \pm 0.7
2017 Dec 14	102.0796	35.125	4.28 \pm 0.11	87.4 \pm 0.7
2017 Dec 14	102.0815	35.144	4.90 \pm 0.10	87.9 \pm 0.6
2017 Dec 14	102.0835	35.162	4.42 \pm 0.10	88.8 \pm 0.6
2017 Dec 14	102.0883	35.207	4.78 \pm 0.13	90.1 \pm 0.8
2017 Dec 14	102.0903	35.227	4.68 \pm 0.13	88.1 \pm 0.8
2017 Dec 14	102.0924	35.246	4.79 \pm 0.10	88.3 \pm 0.6
2017 Dec 14	102.0944	35.266	4.49 \pm 0.11	88.7 \pm 0.7
2017 Dec 14	102.0969	35.290	4.68 \pm 0.26	90.3 \pm 1.6
2017 Dec 14	102.0995	35.314	4.87 \pm 0.17	88.8 \pm 1.0
2017 Dec 14	102.1049	35.365	4.7 \pm 0.7	97.2 \pm 3.9
2017 Dec 14	102.1103	35.417	4.7 \pm 1.0	94.0 \pm 6.0
2017 Dec 14	102.1146	35.458	4.75 \pm 0.30	89.7 \pm 1.9
2017 Dec 14	102.1167	35.478	5.10 \pm 0.26	85.9 \pm 1.5
2017 Dec 14	102.1209	35.518	4.87 \pm 0.26	89.9 \pm 1.5
2017 Dec 14	102.1230	35.538	4.64 \pm 0.26	92.0 \pm 1.7
2017 Dec 14	102.1252	35.559	4.89 \pm 0.19	91.1 \pm 1.1
2017 Dec 14	102.1274	35.580	5.06 \pm 0.19	88.8 \pm 1.1
2017 Dec 14	102.1295	35.600	4.61 \pm 0.27	87.8 \pm 1.8
2017 Dec 14	102.1316	35.620	4.39 \pm 0.43	81.3 \pm 2.6
2017 Dec 14	102.1337	35.640	5.02 \pm 0.52	86.5 \pm 3.0
2017 Dec 14	102.1379	35.681	4.81 \pm 0.21	85.6 \pm 1.2
2017 Dec 14	102.1400	35.701	4.66 \pm 0.18	86.8 \pm 1.1
2017 Dec 14	102.1442	35.742	4.55 \pm 0.25	83.7 \pm 1.5
2017 Dec 14	102.1463	35.762	4.68 \pm 0.27	94.6 \pm 1.6
2017 Dec 14	102.1484	35.782	5.03 \pm 0.22	90.1 \pm 1.3

Table 3 continued

Table 3 (*continued*)

UT Date	JD - 2,458,000	α (°)	P_r (%)	θ_r (°)
2017 Dec 14	102.1504	35.801	5.32 ± 0.22	89.9 ± 1.2
2017 Dec 14	102.1525	35.821	4.88 ± 0.18	87.0 ± 1.0
2017 Dec 14	102.1546	35.841	4.86 ± 0.18	87.1 ± 1.1
2017 Dec 14	102.1566	35.861	4.71 ± 0.14	90.3 ± 0.9
2017 Dec 14	102.1587	35.882	4.58 ± 0.16	87.1 ± 1.0
2017 Dec 14	102.1608	35.902	4.67 ± 0.23	89.0 ± 1.4
2017 Dec 14	102.1629	35.922	5.02 ± 0.28	87.8 ± 1.6
2017 Dec 14	102.1650	35.942	5.36 ± 0.36	91.4 ± 1.9
2017 Dec 14	102.1650	35.942	5.36 ± 0.36	91.4 ± 1.9
2017 Dec 15	102.8832	43.634	8.08 ± 0.14	88.6 ± 0.5
2017 Dec 15	102.8854	43.660	7.89 ± 0.14	88.8 ± 0.5
2017 Dec 15	102.8875	43.686	7.78 ± 0.13	88.0 ± 0.5
2017 Dec 15	102.8891	43.705	7.65 ± 0.13	88.9 ± 0.5
2017 Dec 15	102.8906	43.723	8.24 ± 0.13	88.9 ± 0.5
2017 Dec 15	102.8922	43.742	7.99 ± 0.13	88.1 ± 0.5
2017 Dec 15	102.8937	43.761	8.58 ± 0.13	88.2 ± 0.5
2017 Dec 15	102.8958	43.785	8.18 ± 0.13	88.0 ± 0.5
2017 Dec 15	102.8978	43.810	8.05 ± 0.12	89.7 ± 0.5
2017 Dec 15	102.8993	43.828	8.21 ± 0.12	88.5 ± 0.5
2017 Dec 15	102.9008	43.846	8.13 ± 0.12	89.0 ± 0.5
2017 Dec 15	102.9024	43.865	7.97 ± 0.13	89.2 ± 0.5
2017 Dec 15	102.9040	43.885	8.18 ± 0.13	89.1 ± 0.5
2017 Dec 15	102.9057	43.904	8.39 ± 0.14	88.7 ± 0.5
2017 Dec 15	102.9073	43.924	8.21 ± 0.14	87.2 ± 0.5
2017 Dec 15	102.9089	43.943	8.52 ± 0.13	90.5 ± 0.5
2017 Dec 15	102.9105	43.963	8.18 ± 0.13	88.5 ± 0.5
2017 Dec 15	102.9121	43.982	8.27 ± 0.14	88.3 ± 0.5
2017 Dec 15	102.9169	44.040	8.40 ± 0.15	87.9 ± 0.6
2017 Dec 15	102.9184	44.059	8.22 ± 0.15	87.5 ± 0.6
2017 Dec 15	102.9215	44.096	8.52 ± 0.16	88.4 ± 0.6
2017 Dec 15	102.9230	44.115	8.20 ± 0.18	88.5 ± 0.7
2017 Dec 15	102.9246	44.135	8.79 ± 0.17	88.3 ± 0.6
2017 Dec 15	102.9263	44.154	8.74 ± 0.19	89.5 ± 0.6
2017 Dec 15	102.9278	44.173	8.44 ± 0.21	88.1 ± 0.7
2017 Dec 15	102.9293	44.191	8.62 ± 0.20	89.5 ± 0.7
2017 Dec 15	102.9308	44.210	8.31 ± 0.18	87.3 ± 0.7
2017 Dec 15	102.9324	44.228	8.24 ± 0.17	87.0 ± 0.6
2017 Dec 15	102.9339	44.247	8.20 ± 0.14	87.4 ± 0.5
2017 Dec 15	102.9355	44.266	8.32 ± 0.15	87.5 ± 0.5
2017 Dec 15	102.9370	44.285	8.44 ± 0.15	88.4 ± 0.5
2017 Dec 15	102.9385	44.304	8.39 ± 0.14	88.2 ± 0.5

Table 3 continued

Table 3 (*continued*)

UT Date	JD - 2,458,000	α (°)	P_r (%)	θ_r (°)
2017 Dec 15	102.9401	44.322	8.04 ± 0.14	87.7 ± 0.5
2017 Dec 15	102.9416	44.341	8.72 ± 0.16	88.0 ± 0.5
2017 Dec 15	102.9431	44.360	8.32 ± 0.15	88.1 ± 0.6
2017 Dec 15	102.9447	44.379	8.34 ± 0.18	89.5 ± 0.6
2017 Dec 15	102.9462	44.397	8.14 ± 0.22	87.8 ± 0.7
2017 Dec 15	102.9478	44.417	8.72 ± 0.20	88.8 ± 0.7
2017 Dec 15	102.9494	44.436	7.99 ± 0.22	89.5 ± 0.8
2017 Dec 15	102.9509	44.455	8.9 ± 0.5	87.5 ± 1.3
2017 Dec 15	102.9525	44.474	8.6 ± 0.9	90.3 ± 2.6
2017 Dec 15	102.9541	44.493	8.1 ± 0.6	84.5 ± 2.0
2017 Dec 15	102.9556	44.513	8.36 ± 0.43	89.8 ± 1.5
2017 Dec 15	102.9573	44.533	8.82 ± 0.34	88.3 ± 1.1
2017 Dec 16	103.8763	56.685	13.95 ± 0.39	86.8 ± 0.8
2017 Dec 16	103.8779	56.708	15.44 ± 0.37	86.2 ± 0.7
2017 Dec 16	103.8794	56.730	14.25 ± 0.34	90.1 ± 0.7
2017 Dec 16	103.8810	56.752	15.28 ± 0.31	87.6 ± 0.6
2017 Dec 16	103.8825	56.774	14.98 ± 0.30	87.6 ± 0.6
2017 Dec 16	103.8841	56.797	14.90 ± 0.31	87.8 ± 0.6
2017 Dec 16	103.8857	56.820	14.95 ± 0.38	88.4 ± 0.7
2017 Dec 16	103.8872	56.842	15.10 ± 0.41	86.4 ± 0.8
2017 Dec 16	103.8888	56.865	15.84 ± 0.34	88.7 ± 0.6
2017 Dec 16	103.8904	56.887	15.54 ± 0.32	86.9 ± 0.6
2017 Dec 16	103.8920	56.910	15.32 ± 0.31	88.1 ± 0.6
2017 Dec 16	103.8935	56.932	16.05 ± 0.32	88.8 ± 0.6
2017 Dec 16	103.8951	56.955	14.65 ± 0.32	87.5 ± 0.6
2017 Dec 16	103.8966	56.977	14.99 ± 0.34	88.4 ± 0.7
2017 Dec 16	103.8981	56.999	14.83 ± 0.34	88.2 ± 0.7
2017 Dec 16	103.8997	57.021	14.8 ± 0.5	87.3 ± 0.9
2017 Dec 16	103.9029	57.067	16.3 ± 0.7	88.5 ± 1.2
2017 Dec 16	103.9044	57.090	15.1 ± 0.5	83.7 ± 1.0
2017 Dec 16	103.9060	57.113	14.8 ± 0.5	86.6 ± 0.9
2017 Dec 16	103.9076	57.136	14.86 ± 0.34	87.7 ± 0.7
2017 Dec 16	103.9092	57.158	14.98 ± 0.35	87.9 ± 0.7
2017 Dec 16	103.9108	57.181	16.12 ± 0.43	87.2 ± 0.7
2017 Dec 16	103.9123	57.204	15.02 ± 0.37	87.7 ± 0.7
2017 Dec 16	103.9139	57.226	15.42 ± 0.36	89.1 ± 0.7
2017 Dec 16	103.9154	57.248	15.75 ± 0.37	88.3 ± 0.7
2017 Dec 16	103.9171	57.272	15.55 ± 0.34	87.8 ± 0.6
2017 Dec 16	103.9187	57.295	14.62 ± 0.32	87.4 ± 0.6
2017 Dec 16	103.9203	57.318	14.39 ± 0.33	88.6 ± 0.7
2017 Dec 16	103.9219	57.341	16.04 ± 0.31	92.4 ± 0.6

Table 3 continued

Table 3 (*continued*)

UT Date	JD - 2,458,000	α (°)	P_r (%)	θ_r (°)
2017 Dec 16	103.9234	57.363	15.74 ± 0.30	89.0 ± 0.6
2017 Dec 16	103.9250	57.387	14.88 ± 0.30	88.1 ± 0.6
2017 Dec 16	103.9267	57.410	15.85 ± 0.30	89.2 ± 0.6
2017 Dec 16	103.9283	57.434	15.01 ± 0.29	89.4 ± 0.6
2017 Dec 16	103.9300	57.459	15.50 ± 0.30	86.9 ± 0.6
2017 Dec 16	103.9318	57.484	15.33 ± 0.30	88.9 ± 0.6
2017 Dec 16	103.9334	57.508	14.88 ± 0.30	88.9 ± 0.6
2017 Dec 16	103.9352	57.534	15.25 ± 0.30	87.6 ± 0.6
2017 Dec 16	103.9370	57.560	15.58 ± 0.30	88.9 ± 0.6
2017 Dec 16	103.9387	57.584	14.48 ± 0.30	88.1 ± 0.6
2017 Dec 16	103.9404	57.608	15.70 ± 0.30	88.2 ± 0.5
2017 Dec 16	103.9420	57.632	15.46 ± 0.30	89.5 ± 0.6
2017 Dec 16	103.9437	57.656	15.54 ± 0.31	89.5 ± 0.6
2017 Dec 16	103.9454	57.680	14.81 ± 0.39	89.5 ± 0.8
2017 Dec 16	103.9470	57.704	15.0 ± 0.5	90.6 ± 0.9
2017 Dec 16	103.9487	57.729	15.9 ± 0.5	86.3 ± 0.9
2017 Dec 16	103.9503	57.752	14.8 ± 0.7	88.5 ± 1.3
2017 Dec 16	103.9520	57.777	14.7 ± 0.5	87.4 ± 1.0
2017 Dec 16	103.9540	57.806	15.1 ± 0.6	88.8 ± 1.1
2017 Dec 16	103.9561	57.836	14.1 ± 0.5	88.6 ± 1.1
2017 Dec 16	103.9578	57.860	14.2 ± 0.6	89.5 ± 1.2
2017 Dec 16	103.9594	57.884	14.3 ± 0.9	88.8 ± 1.7
2017 Dec 16	103.9643	57.955	15.5 ± 0.7	86.8 ± 1.2
2017 Dec 16	103.9677	58.004	15.5 ± 0.6	88.6 ± 1.0
2017 Dec 16	103.9698	58.034	15.7 ± 0.8	88.5 ± 1.5
2017 Dec 16	103.9735	58.088	16.8 ± 0.8	88.5 ± 1.4
2017 Dec 16	103.9751	58.112	16.3 ± 1.0	95.6 ± 1.8
2017 Dec 16	103.9768	58.136	15.3 ± 0.6	86.5 ± 1.1
2017 Dec 16	103.9786	58.161	15.0 ± 0.6	89.8 ± 1.2
2017 Dec 16	103.9802	58.185	15.7 ± 0.5	86.2 ± 0.9
2017 Dec 16	103.9819	58.210	15.1 ± 0.6	85.4 ± 1.2
2017 Dec 16	103.9835	58.234	16.3 ± 0.5	87.3 ± 0.9
2017 Dec 16	103.9853	58.259	15.3 ± 0.5	89.1 ± 1.0
2017 Dec 16	103.9870	58.283	15.4 ± 0.8	88.3 ± 1.6
2017 Dec 16	103.9887	58.308	15.1 ± 0.9	85.7 ± 1.6
2017 Dec 16	103.9903	58.332	15.6 ± 1.0	83.7 ± 1.7
2017 Dec 16	103.9962	58.418	16.0 ± 0.8	87.5 ± 1.4
2017 Dec 16	103.9979	58.443	16.1 ± 1.1	91.4 ± 1.8
2017 Dec 16	103.9996	58.467	16.7 ± 0.6	87.8 ± 1.1
2017 Dec 16	104.0013	58.491	15.4 ± 0.5	90.1 ± 0.9
2017 Dec 16	104.0029	58.515	16.70 ± 0.44	89.3 ± 0.8

Table 3 continued

Table 3 (*continued*)

UT Date	JD - 2,458,000	α (°)	P_r (%)	θ_r (°)
2017 Dec 16	104.0045	58.538	14.9 ± 0.5	90.8 ± 0.9
2017 Dec 16	104.0061	58.562	16.28 ± 0.43	89.4 ± 0.8
2017 Dec 16	104.0081	58.590	14.88 ± 0.40	86.4 ± 0.7
2017 Dec 16	104.0102	58.621	17.2 ± 0.6	88.5 ± 0.9
2017 Dec 16	104.0123	58.651	15.2 ± 0.5	88.7 ± 0.9
2017 Dec 16	104.0144	58.682	16.4 ± 0.6	87.4 ± 1.0
2017 Dec 16	104.0165	58.712	14.9 ± 0.8	88.3 ± 1.6
2017 Dec 16	104.0186	58.742	16.3 ± 0.8	86.3 ± 1.3
2017 Dec 16	104.0206	58.772	16.7 ± 0.7	90.6 ± 1.3
2017 Dec 16	104.0227	58.803	16.1 ± 0.5	89.5 ± 1.0
2017 Dec 16	104.0249	58.834	16.1 ± 0.5	88.4 ± 0.8
2017 Dec 16	104.0270	58.865	16.12 ± 0.36	89.2 ± 0.7
2017 Dec 16	104.0291	58.896	15.59 ± 0.37	89.4 ± 0.7
2017 Dec 16	104.0312	58.926	15.87 ± 0.35	89.6 ± 0.6
2017 Dec 16	104.0333	58.957	16.28 ± 0.27	88.2 ± 0.5
2017 Dec 16	104.0354	58.987	16.02 ± 0.33	88.8 ± 0.6
2017 Dec 16	104.0375	59.018	16.54 ± 0.37	89.4 ± 0.6
2017 Dec 16	104.0401	59.056	17.3 ± 0.5	88.8 ± 0.8
2017 Dec 16	104.0427	59.094	17.64 ± 0.43	87.6 ± 0.7
2017 Dec 16	104.0469	59.155	16.75 ± 0.33	89.0 ± 0.6
2017 Dec 16	104.0491	59.186	18.3 ± 0.7	89.1 ± 1.1
2017 Dec 16	104.0512	59.216	17.7 ± 0.8	86.6 ± 1.3
2017 Dec 16	104.0533	59.247	16.3 ± 0.6	90.4 ± 1.0
2017 Dec 17	104.8919	71.510	24.4 ± 0.5	87.9 ± 0.6
2017 Dec 17	104.8934	71.533	23.0 ± 0.5	89.7 ± 0.6
2017 Dec 17	104.8950	71.556	22.20 ± 0.42	89.2 ± 0.5
2017 Dec 17	104.8967	71.581	24.8 ± 0.5	89.4 ± 0.5
2017 Dec 17	104.8982	71.603	23.3 ± 0.5	87.8 ± 0.6
2017 Dec 17	104.8997	71.625	21.6 ± 0.5	88.5 ± 0.6
2017 Dec 17	104.9012	71.647	24.7 ± 0.5	85.9 ± 0.6
2017 Dec 17	104.9028	71.671	22.2 ± 0.5	89.8 ± 0.6
2017 Dec 17	104.9043	71.694	25.7 ± 0.8	87.6 ± 0.8
2017 Dec 17	104.9059	71.717	23.2 ± 0.5	87.4 ± 0.6
2017 Dec 17	104.9074	71.739	24.2 ± 0.5	88.5 ± 0.5
2017 Dec 17	104.9089	71.761	22.66 ± 0.41	89.4 ± 0.5
2017 Dec 17	104.9105	71.785	24.6 ± 0.5	88.6 ± 0.5
2017 Dec 17	104.9122	71.810	23.5 ± 0.5	86.6 ± 0.6
2017 Dec 17	104.9137	71.832	22.2 ± 1.0	86.6 ± 1.2
2017 Dec 17	104.9420	72.251	21.3 ± 0.9	88.7 ± 1.2
2017 Dec 17	104.9443	72.284	25.9 ± 1.4	81.5 ± 1.5
2017 Dec 17	104.9465	72.317	22.6 ± 0.7	89.4 ± 0.9

Table 3 continued

Table 3 (*continued*)

UT Date	JD - 2,458,000	α (°)	P_r (%)	θ_r (°)
2017 Dec 17	104.9481	72.340	22.7 ± 1.2	82.7 ± 1.4
2017 Dec 17	104.9569	72.470	26.7 ± 0.7	86.8 ± 0.7
2017 Dec 17	104.9695	72.655	26.2 ± 0.6	87.6 ± 0.7
2017 Dec 17	104.9712	72.680	25.0 ± 1.3	90.9 ± 1.5
2017 Dec 17	104.9730	72.706	25.8 ± 0.7	86.7 ± 0.8
2017 Dec 17	104.9770	72.765	25.6 ± 1.4	82.0 ± 1.5
2017 Dec 17	104.9805	72.817	22.2 ± 0.7	89.1 ± 0.9
2017 Dec 17	104.9866	72.906	23.8 ± 1.1	89.9 ± 1.3
2017 Dec 17	104.9903	72.961	24.1 ± 0.7	90.6 ± 0.8
2017 Dec 17	104.9921	72.987	22.58 ± 0.42	89.8 ± 0.5
2017 Dec 17	104.9961	73.045	24.7 ± 0.6	90.1 ± 0.7
2017 Dec 17	105.0000	73.104	22.8 ± 0.5	90.5 ± 0.6
2017 Dec 17	105.0018	73.130	24.6 ± 0.6	87.4 ± 0.7
2017 Dec 17	105.0036	73.156	25.2 ± 0.6	92.4 ± 0.7
2017 Dec 17	105.0054	73.182	23.7 ± 0.5	89.7 ± 0.6
2017 Dec 17	105.0072	73.208	26.6 ± 0.7	88.0 ± 0.7
2017 Dec 17	105.0090	73.235	25.8 ± 0.6	88.2 ± 0.7
2017 Dec 17	105.0107	73.260	22.9 ± 0.5	80.2 ± 0.5
2017 Dec 17	105.0123	73.283	25.8 ± 0.6	87.3 ± 0.7
2017 Dec 17	105.0140	73.309	27.6 ± 1.3	94.8 ± 1.3
2017 Dec 17	105.0179	73.366	28.5 ± 1.2	85.6 ± 1.2
2017 Dec 17	105.0218	73.422	25.3 ± 1.0	86.0 ± 1.1
2017 Dec 17	105.0236	73.448	28.7 ± 0.9	89.3 ± 0.9
2017 Dec 18	105.8704	85.195	31.6 ± 0.5	88.7 ± 0.5
2017 Dec 18	105.8725	85.223	31.7 ± 0.5	88.2 ± 0.5
2017 Dec 18	105.8745	85.250	31.9 ± 0.5	87.4 ± 0.4
2017 Dec 18	105.8766	85.277	31.2 ± 0.5	88.5 ± 0.4
2017 Dec 18	105.8787	85.305	31.1 ± 0.5	88.5 ± 0.4
2017 Dec 18	105.8808	85.333	32.46 ± 0.43	88.1 ± 0.4
2017 Dec 18	105.8828	85.360	32.27 ± 0.42	88.6 ± 0.4
2017 Dec 18	105.8848	85.386	32.43 ± 0.41	88.7 ± 0.4
2017 Dec 18	105.8868	85.413	31.90 ± 0.39	88.6 ± 0.4
2017 Dec 18	105.8889	85.440	31.2 ± 0.5	88.7 ± 0.4
2017 Dec 18	105.8909	85.467	31.85 ± 0.38	88.4 ± 0.4
2017 Dec 18	105.8951	85.523	31.73 ± 0.38	88.0 ± 0.3
2017 Dec 18	105.8972	85.550	31.37 ± 0.38	88.8 ± 0.4
2017 Dec 18	105.8992	85.577	30.69 ± 0.39	89.2 ± 0.4
2017 Dec 18	105.9013	85.604	30.76 ± 0.39	89.0 ± 0.4
2017 Dec 18	105.9033	85.631	31.29 ± 0.42	88.2 ± 0.4
2017 Dec 18	105.9054	85.659	31.6 ± 0.5	88.5 ± 0.4
2017 Dec 18	105.9078	85.690	32.1 ± 0.5	88.0 ± 0.4

Table 3 continued

Table 3 (*continued*)

UT Date	JD - 2,458,000	α ($^{\circ}$)	P_r (%)	θ_r ($^{\circ}$)
2017 Dec 18	105.9100	85.719	31.4 ± 0.5	88.1 ± 0.5
2017 Dec 18	105.9121	85.746	31.1 ± 0.5	87.7 ± 0.5
2017 Dec 18	105.9142	85.774	32.2 ± 0.6	88.5 ± 0.5
2017 Dec 18	105.9162	85.802	32.1 ± 0.6	89.0 ± 0.5
2017 Dec 18	105.9184	85.829	31.0 ± 0.6	92.3 ± 0.5
2017 Dec 18	105.9204	85.856	32.0 ± 0.5	87.8 ± 0.5
2017 Dec 18	105.9224	85.883	31.8 ± 0.5	88.7 ± 0.5
2017 Dec 18	105.9244	85.909	30.6 ± 0.5	88.2 ± 0.5
2017 Dec 18	105.9264	85.935	32.2 ± 0.5	88.7 ± 0.5
2017 Dec 18	105.9284	85.961	31.9 ± 0.5	89.0 ± 0.5
2017 Dec 18	105.9304	85.988	32.1 ± 0.5	88.9 ± 0.5
2017 Dec 18	105.9324	86.014	30.9 ± 0.5	88.2 ± 0.5
2017 Dec 18	105.9344	86.039	30.8 ± 0.6	88.9 ± 0.5
2017 Dec 18	105.9364	86.066	29.8 ± 0.8	87.5 ± 0.7
2017 Dec 18	105.9384	86.092	31.3 ± 0.9	87.8 ± 0.8
2017 Dec 18	105.9404	86.118	30.8 ± 0.8	87.8 ± 0.7
2017 Dec 18	105.9424	86.144	29.6 ± 0.7	88.6 ± 0.7
2017 Dec 18	105.9444	86.171	32.0 ± 0.7	88.9 ± 0.6
2017 Dec 18	105.9464	86.197	31.5 ± 0.7	88.7 ± 0.6
2017 Dec 18	105.9484	86.223	31.3 ± 0.6	89.1 ± 0.6
2017 Dec 18	105.9504	86.250	32.5 ± 0.7	89.2 ± 0.6
2017 Dec 18	105.9525	86.276	31.7 ± 0.7	88.9 ± 0.6
2017 Dec 18	105.9545	86.303	29.6 ± 0.7	88.7 ± 0.6
2017 Dec 18	105.9565	86.329	31.4 ± 0.7	91.5 ± 0.6
2017 Dec 18	105.9585	86.356	30.4 ± 0.6	88.7 ± 0.6
2017 Dec 18	105.9606	86.382	32.0 ± 0.6	88.1 ± 0.5
2017 Dec 18	105.9627	86.410	31.2 ± 0.6	88.3 ± 0.5
2017 Dec 18	105.9647	86.436	31.0 ± 0.5	88.6 ± 0.5
2017 Dec 18	105.9668	86.463	31.3 ± 0.5	89.3 ± 0.5
2017 Dec 18	105.9688	86.489	30.7 ± 0.5	88.2 ± 0.5
2017 Dec 18	105.9708	86.515	32.9 ± 0.5	89.0 ± 0.5
2017 Dec 18	105.9729	86.542	30.2 ± 0.5	88.9 ± 0.5
2017 Dec 18	105.9749	86.569	32.4 ± 0.5	88.0 ± 0.5
2017 Dec 18	105.9770	86.596	32.8 ± 0.6	89.2 ± 0.6
2017 Dec 18	105.9790	86.622	31.7 ± 0.6	88.6 ± 0.5
2017 Dec 18	105.9811	86.649	31.7 ± 0.5	88.7 ± 0.5
2017 Dec 18	105.9832	86.676	33.1 ± 0.5	89.2 ± 0.5
2017 Dec 18	105.9853	86.703	33.8 ± 0.5	89.9 ± 0.5
2017 Dec 18	105.9873	86.730	30.7 ± 0.5	89.6 ± 0.5
2017 Dec 18	105.9894	86.756	33.2 ± 0.6	89.7 ± 0.5
2017 Dec 18	105.9914	86.783	33.5 ± 0.6	89.0 ± 0.5

Table 3 continued

Table 3 (*continued*)

UT Date	JD - 2,458,000	α ($^{\circ}$)	P_r (%)	θ_r ($^{\circ}$)
2017 Dec 18	105.9936	86.810	33.6 ± 0.6	88.7 ± 0.5
2017 Dec 18	105.9956	86.837	34.7 ± 0.7	89.5 ± 0.5
2017 Dec 18	105.9977	86.863	33.0 ± 0.7	88.6 ± 0.6
2017 Dec 18	105.9997	86.890	32.5 ± 0.6	88.1 ± 0.6
2017 Dec 18	106.0019	86.918	33.2 ± 0.6	88.4 ± 0.6
2017 Dec 19	106.8743	97.169	35.3 ± 0.9	86.4 ± 0.7
2017 Dec 19	106.8764	97.191	36.4 ± 0.9	88.3 ± 0.7
2017 Dec 19	106.8784	97.213	38.9 ± 1.0	87.9 ± 0.7
2017 Dec 19	106.8804	97.234	38.0 ± 0.9	88.3 ± 0.7
2017 Dec 19	106.8823	97.256	37.8 ± 0.9	88.5 ± 0.7
2017 Dec 19	106.8843	97.277	35.9 ± 0.9	88.4 ± 0.7
2017 Dec 19	106.8863	97.299	37.4 ± 0.9	87.0 ± 0.7
2017 Dec 19	106.8884	97.321	35.8 ± 0.9	89.4 ± 0.8
2017 Dec 19	106.8924	97.364	40.2 ± 1.1	88.5 ± 0.8
2017 Dec 19	106.8944	97.386	37.4 ± 1.1	90.1 ± 0.8
2017 Dec 19	106.8964	97.408	40.2 ± 1.1	89.6 ± 0.8
2017 Dec 19	106.8984	97.429	42.0 ± 1.2	88.4 ± 0.8
2017 Dec 19	106.9011	97.458	39.0 ± 1.1	87.4 ± 0.8
2017 Dec 19	106.9038	97.487	40.7 ± 1.3	89.7 ± 0.9
2017 Dec 19	106.9078	97.530	37.2 ± 1.2	88.0 ± 1.0
2017 Dec 19	106.9098	97.551	37.2 ± 1.3	88.9 ± 1.0
2017 Dec 19	106.9118	97.573	40.1 ± 1.4	88.5 ± 1.0
2017 Dec 19	106.9159	97.616	35.3 ± 1.2	87.4 ± 1.0
2017 Dec 19	106.9178	97.637	37.9 ± 1.3	89.7 ± 1.0
2017 Dec 19	106.9199	97.659	38.9 ± 1.3	87.2 ± 1.0
2017 Dec 19	106.9219	97.681	39.0 ± 1.3	88.4 ± 1.0
2017 Dec 19	106.9239	97.702	40.9 ± 1.4	82.7 ± 1.0
2017 Dec 19	106.9280	97.745	36.1 ± 1.1	94.6 ± 0.9
2017 Dec 19	106.9299	97.767	37.7 ± 1.2	87.8 ± 0.9
2017 Dec 19	106.9319	97.788	37.5 ± 1.2	89.9 ± 0.9
2017 Dec 19	106.9340	97.809	39.4 ± 1.1	89.5 ± 0.9
2017 Dec 19	106.9360	97.831	40.4 ± 1.1	89.5 ± 0.8
2017 Dec 19	106.9380	97.852	39.0 ± 1.0	89.9 ± 0.7
2017 Dec 19	106.9400	97.874	39.0 ± 0.9	87.9 ± 0.7
2017 Dec 19	106.9420	97.895	37.9 ± 0.9	87.5 ± 0.7
2017 Dec 19	106.9441	97.917	38.8 ± 0.9	88.5 ± 0.7
2017 Dec 19	106.9461	97.938	38.8 ± 0.9	86.9 ± 0.7
2017 Dec 19	106.9481	97.960	37.0 ± 0.8	88.6 ± 0.7
2017 Dec 19	106.9501	97.981	35.8 ± 1.0	88.0 ± 0.8
2017 Dec 19	106.9523	98.004	39.1 ± 1.0	88.9 ± 0.7
2017 Dec 19	106.9544	98.026	37.8 ± 1.0	89.9 ± 0.8

Table 3 continued

Table 3 (*continued*)

UT Date	JD - 2,458,000	α (°)	P_r (%)	θ_r (°)
2017 Dec 19	106.9565	98.048	36.6 ± 1.2	87.8 ± 1.0
2017 Dec 19	106.9586	98.071	35.4 ± 1.2	90.8 ± 1.0
2017 Dec 19	106.9608	98.094	38.2 ± 1.3	88.1 ± 1.0
2017 Dec 19	106.9630	98.117	39.1 ± 1.8	88.8 ± 1.4
2017 Dec 19	106.9655	98.143	37.1 ± 1.9	86.2 ± 1.5
2017 Dec 19	106.9676	98.166	35.0 ± 2.0	90.0 ± 1.7
2017 Dec 19	106.9698	98.189	37.5 ± 2.1	91.1 ± 1.6
2017 Dec 19	106.9722	98.214	34.7 ± 1.9	89.9 ± 1.6
2017 Dec 20	107.8607	106.552	43.1 ± 2.7	90.0 ± 1.9
2017 Dec 20	107.8641	106.581	41.6 ± 3.3	88.7 ± 2.3
2017 Dec 20	107.8675	106.609	46.3 ± 3.8	91.4 ± 2.4
2017 Dec 20	107.8708	106.637	49.8 ± 4.9	88.6 ± 2.9
2017 Dec 20	107.8742	106.666	44.1 ± 3.3	84.3 ± 2.1
2017 Dec 20	107.8809	106.723	43.8 ± 3.4	87.8 ± 2.2
2017 Dec 20	107.8843	106.751	42.0 ± 2.9	90.7 ± 2.0
2017 Dec 20	107.8876	106.780	44.8 ± 3.2	89.6 ± 2.1
2017 Dec 20	107.8910	106.808	38.9 ± 2.8	90.0 ± 2.1
2017 Dec 20	107.8944	106.837	37.9 ± 3.1	92.7 ± 2.4
2017 Dec 20	107.8978	106.865	38.9 ± 2.9	87.6 ± 2.2
2017 Dec 20	107.9011	106.894	35.9 ± 3.5	88.4 ± 2.9
2017 Dec 20	107.9045	106.922	43.9 ± 4.6	87.4 ± 3.1
2017 Dec 20	107.9113	106.979	37.7 ± 4.0	92.1 ± 3.1
2017 Dec 20	107.9147	107.007	37.3 ± 3.6	92.4 ± 2.8
2017 Dec 20	107.9181	107.036	40.4 ± 3.5	91.3 ± 2.5
2017 Dec 20	107.9215	107.064	36.5 ± 3.1	87.3 ± 2.5
2017 Dec 20	107.9249	107.093	44.6 ± 3.5	90.4 ± 2.3
2017 Dec 20	107.9317	107.149	36.6 ± 3.0	89.8 ± 2.4
2017 Dec 20	107.9351	107.178	39.2 ± 3.1	88.1 ± 2.3
2017 Dec 21	108.8691	114.041	46.7 ± 4.6	91.3 ± 2.9
2017 Dec 21	108.8753	114.082	47.7 ± 5.6	88.4 ± 3.4
2017 Dec 21	108.8815	114.123	54.4 ± 5.8	88.8 ± 3.1
2017 Dec 21	108.8877	114.164	50.2 ± 3.5	89.5 ± 2.0
2017 Dec 21	108.8939	114.205	45.4 ± 2.7	90.7 ± 1.7
2017 Dec 21	108.9001	114.246	38.7 ± 1.9	88.1 ± 1.4
2017 Dec 21	108.9063	114.286	43.7 ± 2.6	85.2 ± 1.7

NOTE— JD is Julian date at the middle time of each sequence. α is the solar phase angle of Phaethon. P_r and θ_r are the degree of linear polarization and position angle in the scattering plane, respectively.